

การพัฒนาโฟโตแคปเปลอร์ชนิดฟิล์มบาง
ซึ่งประกอบด้วยไดโอดเปล่งแสงชนิดอะมอร์ฟัสซิลิคอนคาร์ไบด์
และโฟโตไดโอดชนิดอะมอร์ฟัสซิลิคอนเจอร์เมเนียม



นางสาวพนทิพย์ วงศ์วรรณ

วิทยานิพนธ์นี้เป็นส่วนหนึ่งของการศึกษาตามหลักสูตรปริญญาวิศวกรรมศาสตรมหาบัณฑิต

สาขาวิชาวิศวกรรมไฟฟ้า ภาควิชาวิศวกรรมไฟฟ้า

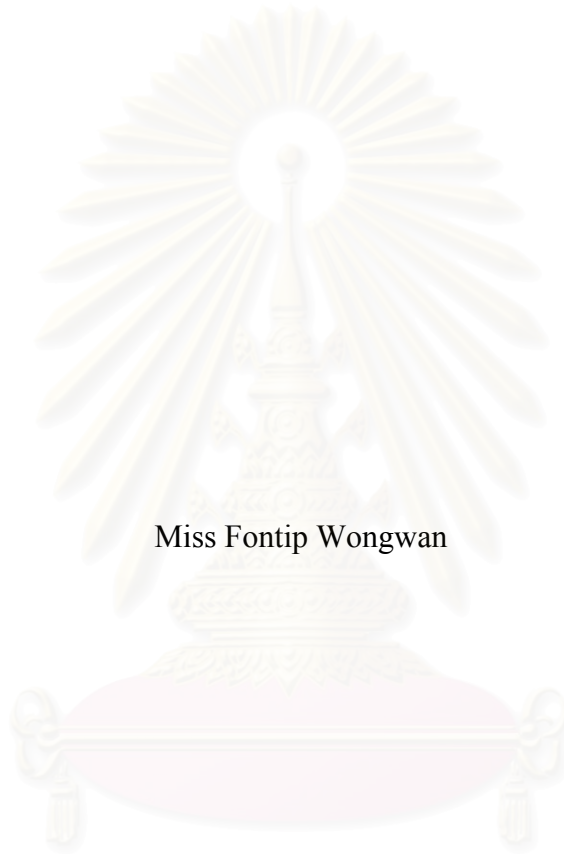
คณะวิศวกรรมศาสตร์ จุฬาลงกรณ์มหาวิทยาลัย

ปีการศึกษา 2543

ISBN 974-346-389-5

ลิขสิทธิ์ของจุฬาลงกรณ์มหาวิทยาลัย

**DEVELOPMENT OF THIN FILM PHOTOCOUPLER
CONSISTING OF AMORPHOUS SILICON CARBIDE LIGHT EMITTING DIODE
AND AMORPHOUS SILICON GERMANIUM PHOTODIODE**



Miss Fontip Wongwan

สถาบันวิทยบริการ
จุฬาลงกรณ์มหาวิทยาลัย

A Thesis Submitted in Partial Fulfillment of the Requirements
for the Degree of Master of Engineering in Electrical Engineering
Department of Electrical Engineering

Faculty of Engineering
Chulalongkorn University

Academic Year 2000

ISBN 974-346-389-5

| | |
|----------------|---|
| Thesis Title | Development of Thin Film Photocoupler Consisting of Amorphous Silicon Carbide Light Emitting Diode and Amorphous Silicon Germanium Photodiode |
| By | Miss Fontip Wongwan |
| Department | Electrical Engineering |
| Thesis Advisor | Associate Professor Dr. Dusit Kruangam |

Accepted by the Faculty of Engineering, Chulalongkorn University, in Partial Fulfillment of the Requirements for the Master's Degree.

..... Dean of Faculty of Engineering
(Professor Dr. Somsak Panyakeow)

Thesis Committee

..... Chairman
(Professor Dr. Somsak Panyakeow)

..... Thesis Advisor
(Associate Professor Dr. Dusit Kruangam)

..... Member
(Associate Professor Dr. Montri Sawadsaringkarn)

..... Member
(Associate Professor Dr. Koarakot Wattanavichean)

..... Member
(Dr. Porpon Sitchanugritst)

ฝนทิพย์ วงศ์วรรณ: การพัฒนาโฟโตคัปเปิลอร์ชนิดฟิล์มบางซึ่งประกอบด้วย ไดโอดเปล่งแสงชนิดอะมอร์ฟัสซิลิคอนคาร์ไบด์และโฟโตไดโอดชนิดอะมอร์ฟัสซิลิคอนเจอร์เมเนียม (DEVELOPMENT OF THIN PHOTOCOUPLER CONSISTING OF AMORPHOUS SILICON CARBIDE LIGHT EMITTING DIODE AND AMORPHOUS SILICON GERMANIUM) อาจารย์ที่ปรึกษา: รศ.ดร. คุณิต เครื่องงาม, 66 หน้า, ISBN 974-346-389-5

วิทยานิพนธ์ฉบับนี้ รายงานผลการพัฒนาโฟโตคัปเปิลอร์ชนิดฟิล์มบางซึ่งประกอบด้วย ภาวเปล่งแสงที่ประดิษฐ์จากไดโอดเปล่งแสงชนิดอะมอร์ฟัสซิลิคอนคาร์ไบด์ และภาวรับแสงที่ประดิษฐ์จากโฟโตไดโอดและโฟโตริซิซิสเตอร์ชนิดอะมอร์ฟัสซิลิคอนเจอร์เมเนียม โฟโตคัปเปิลอร์นี้ได้รับการออกแบบให้สามารถทำงานด้วยแสงย่านอินฟราเรด

ฟิล์มบางอะมอร์ฟัสซิลิคอนเจอร์เมเนียมเตรียมด้วยวิธีการแยกสลายก๊าซด้วยประจุเรืองแสง โดยใช้ก๊าซผสมของไซเลน (SiH_4) และเจอร์แมน (GeH_4) เป็นก๊าซเริ่มต้น งานวิจัยเริ่มจากการติดตั้งระบบก๊าซ GeH_4 และศึกษาการหาเงื่อนไขการปลูกฟิล์มบางเพื่อให้ได้ฟิล์มบางอะมอร์ฟัสซิลิคอนเจอร์เมเนียมที่มีค่าสภาพนำไฟฟ้าด้วยแสงที่ดีที่สุด ผลการศึกษาพบว่า เมื่อเพิ่มปริมาณก๊าซ GeH_4 จะทำให้ช่องว่างพลังงานของฟิล์มบางแคบลง และอุณหภูมิแผ่นที่เหมาะสมที่สุดคือ 250 องศาเซลเซียส นอกจากนี้ยังพบว่า การผสมก๊าซไฮโดรเจน (H_2) ด้วยปริมาณที่เหมาะสมก็เป็นเงื่อนไขที่สำคัญมาก ผลการทดลองทำให้สามารถเตรียมฟิล์มบางอะมอร์ฟัสซิลิคอนเจอร์เมเนียมที่มีค่าช่องว่างพลังงานช่วง 1.4–1.6 eV ที่มีค่าสภาพนำไฟฟ้าด้วยแสงระดับ 10^{-4} - 10^{-6} S/cm ต่อจากนั้นได้ประดิษฐ์โฟโตไดโอดชนิดอะมอร์ฟัสซิลิคอนเจอร์เมเนียมรอยต่อ p-i-n และได้ผลว่าสามารถตอบสนองต่อแสงย่านอินฟราเรดได้ดี

โฟโตไดโอดชนิดอะมอร์ฟัสซิลิคอนเจอร์เมเนียมที่พัฒนาขึ้นดังกล่าว ถูกนำไปประยุกต์ใช้งานในโฟโตคัปเปิลอร์ซึ่งมีภาวเปล่งแสงเป็นไดโอดเปล่งแสงชนิดอะมอร์ฟัสซิลิคอนคาร์ไบด์ ผลการประดิษฐ์โฟโตคัปเปิลอร์ปรากฏว่า โฟโตคัปเปิลอร์นี้สามารถทำงานด้วยแสงย่านอินฟราเรด ช่วงความยาวคลื่น 700-900 นาโนเมตรได้ดี อัตราส่วนของการถ่ายทอดกระแสของโฟโตคัปเปิลอร์มีค่าระดับ $10^{-4}\%$ โฟโตคัปเปิลอร์ชนิดอะมอร์ฟัสที่พัฒนาขึ้นในวิทยานิพนธ์นี้มีศักยภาพในการนำไปประยุกต์ใช้งานเป็นอุปกรณ์อิเล็กทรอนิกส์ต่างๆ อาทิ เครื่องวัดจำนวนของวัสดุ เครื่องวัดขนาด และรูปร่างของวัสดุ การสื่อสารด้วยแสง อุตสาหกรรมการวัดคุม และอุปกรณ์ออปโตอิเล็กทรอนิกส์ต่างๆ เป็นต้น

ภาควิชา วิศวกรรมไฟฟ้า

สาขาวิชา วิศวกรรมไฟฟ้า

ปีการศึกษา 2543

ลายมือชื่อนิสิต _____

ลายมือชื่ออาจารย์ที่ปรึกษา _____

ลายมือชื่ออาจารย์ที่ปรึกษาร่วม _____ -

FONTIP WONGWAN: DEVELOPMENT OF THIN FILM PHOTOCOUPLER CONSISTING OF AMORPHOUS SILICON CARBIDE LIGHT EMITTING DIODE AND AMORPHOUS SILICON GERMANIUM PHOTODIODE. THESIS ADVISOR: ASSOCIATE PROF. DR. DUSIT KRUANGAM, 66 pp., ISBN 974-346-389-5.

Amorphous thin film photocouplers consisting of amorphous silicon carbide (a-SiC:H) thin film light emitting diodes and amorphous silicon germanium (a-SiGe:H) thin film photodiodes and photoresistors have been developed. The amorphous photocouplers are designed for operation in the infrared regions.

The a-SiGe:H thin films were prepared by the glow discharge plasma CVD method from the gas mixture of silane (SiH₄) and germane (GeH₄). The research started from the installation of GeH₄ gas line system, followed by the optimizations of preparation conditions for obtaining high photo-conductivity undoped a-SiGe:H films. The results showed that the optical energy gap of a-SiGe:H decreased when the flow rate of GeH₄ increased, and the optimal substrate temperature was about 250 °C. It was also found that the dilution of hydrogen gas (H₂) with an appropriate flow rate was another important factor to obtain high photo-conductivity a-SiGe:H. In the work, a-SiGe:H having high photo-conductivity (10⁻⁶-10⁻⁴ S/cm) and small optical energy gaps of 1.4 –1.6 eV were prepared. The amorphous p-i-n junction photodiodes, using the a-SiGe:H as active layers, were fabricated and had good responses to the infrared light.

The developed a-SiGe:H thin film photodiodes were applied as the light detectors in the amorphous photocouplers. The results showed that the photocouplers could be operated in the infrared light (wavelength 700 – 900 nanometer). The current transfer ratio of the photocoupler was in the order of 10⁻⁴ %. The amorphous photocouplers have potentials to be used in various electronics applications; for examples, measurement of material sizes, optical communication, and optoelectronics, etc.

Department Electrical Engineering
 Field of Study Electrical Engineering
 Academic Year 2000

Student's signature-----
 Advisor's signature-----
 Co-advisor's signature -----

ACKNOWLEDGEMENT

This work has been done at the Semiconductor Device Research Laboratory (SDRL), Department of Electrical Engineering, Faculty of Engineering, Chulalongkorn University under the supervision of Associate Professor Dr. Dusit Kruangam.

The author would like to express the greatest acknowledge to the supervisor, Associate Professor Dr. Dusit Kruangam for providing the opportunity to do this research in the laboratory with the valuable guidance.

The author wishes to make deep acknowledgement to the members of the Thesis Committee: Professor Dr. Somsak Panyakeow, Associate Professor Dr. Montri Sawadsaringkarn, Associate Professor Dr. Koarakot Wattanavichean (Kasetsart University), Dr. Porpon Sitchanugrist (National Electronics and Computer Technology Center) and Associate Professor Dr. Dusit Kruangam for the critical reading, useful discussion and guidance.

The special thank is concerned to Mr. Kriengkrai Chirakawikul for instructing the author to do experiments required in the thesis.

The author also gratefully thanks to the staffs in SDRL for providing help while doing the research: Dr. Suwat Sopitpan, Mr. Supachok Thainoi, Mrs. Kwanruan Thainoi, Mr. Pornchai Changmuang. In addition, the appreciated thanks are concerned to Dr. Arporn Teeramongkonrasmee and Dr. Songphol Kanjanachuchai for suggestion on this thesis and Mr. Tula Chutarosaka for valuable help while doing the experiments.

This work was supported by (1) Energy Conservation Promotion Fund, National Energy Policy Office (NEPO), (2) Thailand Graduate Institute of Science and Technology, NSTDA and (3) Career Development Program, National Science and Technology Development Agency (NSTDA).

Finally, the author wishes to thank her family for the endless and warm encouragement.

CONTENTS

| | Page |
|--|------|
| Abstract (Thai) | iv |
| Abstract (English) | v |
| Acknowledgement | vi |
| Contents | vii |
| List of Figures | x |
| List of Tables | xiii |
| CHAPTER | |
| 1 Introduction | 1 |
| 1.1 Background | 1 |
| 1.2 Objectives | 3 |
| 1.3 Structure of the Thesis | 3 |
| 2 Preparation of Hydrogenated Amorphous Silicon Germanium by Glow Discharge Plasma CVD Method | 5 |
| 2.1 Introduction | 5 |
| 2.2 Preparation of a-SiGe:H by the Glow Discharge Plasma CVD System | 5 |
| 2.2.1 Structure of the Glow Discharge Plasma CVD System | 7 |
| 2.2.2 Preparation of Substrates | 8 |
| 2.2.3 Deposition of a-SiGe:H | 9 |
| 3 Basic Properties of Undoped a-SiGe:H | 11 |
| 3.1 Introduction | 11 |
| 3.2 Structural Properties of a-SiGe:H | 11 |
| 3.2.1 Measurement of Germanium Contents in a-SiGe:H by Infrared Transmittance Spectra | 12 |
| 3.2.2 Measurement of Dangling Bond Density in a-SiGe:H by Electron Spin Resonance (ESR) | 14 |
| 3.3 Optical Properties of a-SiGe:H | 16 |
| 3.4 Electrical Properties of a-SiGe:H | 18 |

CONTENTS (continued)

CHAPTER

| | | |
|---|---|----|
| 4 | Improvement of Optoelectronics Properties of a-SiGe:H | 23 |
| | 4.1 Introduction | 23 |
| | 4.2 Improvement Photo-conductivity of a-SiGe:H by the Optimization of Substrate Temperature | 23 |
| | 4.3 Improvement of Photo-conductivity of a-SiGe:H by the Optimization of Gas Flow Rate Ratio of $H_2/(GeH_4+SiH_4)$... | 26 |
| 5 | Structure and Fabrication of the Infrared-Light a-SiGe:H Thin Film Photodiode | 31 |
| | 5.1 Introduction | 31 |
| | 5.2 Structure of the a-SiGe:H Thin Film Photodiode | 31 |
| | 5.3 Fabrication of a-SiGe:H Thin Film Photodiodes | 32 |
| | 5.4 Basic Output Characteristics of a-SiGe:H Thin Film Photodiodes | 34 |
| 6 | Structure and Fabrication of Amorphous Photocouplers Consisting of a-SiC:H Light Emitting Diode and a-SiGe:H Photodiode | 39 |
| | 6.1 Introduction | 39 |
| | 6.2 Usefulness of Photocouplers | 40 |
| | 6.3 Structures of Conventional Amorphous Thin Film Photocouplers | 41 |
| | 6.4 Development of a-SiC:H/a-SiGe:H Photocouplers | 43 |
| | 6.4.1 Fabrication of a-SiC:H Thin Film Light Emitting Diodes | 46 |
| | 6.4.2 Fabrication of a-SiC:H Thin Film Photodiodes | 50 |
| | 6.5 Basic Characteristics of a-SiC:H/a-SiGe:H Thin Film Photocouplers | 51 |
| 7 | Conclusions | 55 |

CONTENTS (continued)

| | | |
|---|--|----|
| References | | 57 |
| List of Publications | | 60 |
| Appendix Fabrication of Amorphous Silicon Germanium Solar Cell | | 62 |
| 1 Introduction | | 62 |
| 2 Structure and Fabrication of a-SiGe:H Solar Cell | | 63 |
| 3 Results | | 64 |
| Biography | | 66 |



สถาบันวิทยบริการ
จุฬาลงกรณ์มหาวิทยาลัย

LIST OF FIGURES

| Figures | Page |
|---|------|
| 1.1 Picture of a-Si:H and other alloys deposited on glass substrates | 2 |
| 2.1 Schematic diagram of the glow discharge plasma CVD system | 7 |
| 2.2 Photographs of the glow discharge plasma CVD system at the Semiconductor Device Research Laboratory, Chulalongkorn University (a) reaction chamber and (b) partial part of gas system | 8 |
| 2.3 Deposition process of a-SiGe:H by the glow discharge plasma CVD | 9 |
| 3.1 An example of infrared transmittance spectrum for an a-SiGe:H film prepared at the gas flow rate ratio $\text{GeH}_4/(\text{GeH}_4+\text{SiH}_4) \times = 0.09$ | 12 |
| 3.2 The calculation of IR absorption coefficient of a-SiGe:H from the spectrum of IR transmittance (a) Simplified diagram for IR absorption measurement (b) Spectrum of IR transmittance | 13 |
| 3.3 Infrared absorption coefficient spectrum of Ge-H atom of a-SiGe:H (stretching mode) | 14 |
| 3.4 Relationship between ESR spin density and gas flow rate for a-SiGe:H | 15 |
| 3.5 The optical absorption coefficient spectra near the fundamental band edge of a-SiGe:H. The parameter (x) is the $\text{GeH}_4/(\text{GeH}_4+\text{SiH}_4)$ gas flow ratio... | 16 |
| 3.6 Tauc's plot for the determination of the optical energy gap of a-SiGe:H ... | 17 |
| 3.7 Relationship between the GeH_4 gas fraction (x) and the optical energy gap of undoped a-SiGe:H | 17 |
| 3.8 Schematic diagrams of the measurements of (a) dark-conductivity and (b) photo-conductivity for a-SiGe:H | 19 |
| 3.9 Relationship between dark-conductivity (σ_D), photo-conductivity (σ_{ph}) and the ratio of σ_{ph}/σ_D for a-SiGe:H prepared by different gas flow rate ratio ($\text{GeH}_4/(\text{GeH}_4+\text{SiH}_4)$) | 20 |
| 3.10 Relationship between the conductivities and the optical energy gaps for undoped a-SiGe:H | 21 |

LIST OF FIGURES (continued)

Figures

| | | |
|-----|---|----|
| 4.1 | Relationship between conductivity of a-SiGe:H and substrate temperature | 24 |
| 4.2 | Dependence of the optical energy gap of undoped a-SiGe:H on the substrate temperature | 25 |
| 4.3 | Relationship between conductivity and H ₂ ratio of a-SiGe:H | 28 |
| 4.4 | Dependence of the optical energy gap of undoped a-SiGe:H on H ₂ gas flow rate ratio | 28 |
| 4.5 | Relationship between the ratio of σ_{ph}/σ_D and the optical energy gap of undoped a-SiGe:H | 29 |
| 5.1 | Basic structure of the a-SiGe:H thin film photodiode | 31 |
| 5.2 | Fabrication process of the a-SiGe:H thin film photodiode | 33 |
| 5.3 | Picture of a-SiGe:H photodiodes | 33 |
| 5.4 | Examples of I-V curves of two a-SiGe:H thin film photodiodes having different optical energy gaps of a-SiGe:H. E _{opt} denotes the optical energy gap of a-SiGe:H in the i-layer | 34 |
| 5.5 | Schematic band diagrams of a-SiGe:H TFPD (a) equilibrium (b) weak reverse bias and (c) strong reverse bias condition | 36 |
| 6.1 | Pictures of conventional crystalline photocouplers | 41 |
| 6.2 | Structures of a-SiC:H/a-Si:H photocouplers | 42 |
| 6.3 | Examples of packages of amorphous photocouplers | 42 |
| 6.4 | Pictures of a-SiC:H/a-Si:H photocouplers | 43 |
| 6.5 | Structures of amorphous photocouplers having an a-SiC:H TFLED as a red color-near infrared light emitting device. Type (a) uses a-SiGe:H thin film photodiode as a light detector. Type (b) uses a-SiGe:H photoresistor as light detector | 45 |
| 6.6 | Structure of amorphous silicon carbide (a-SiC:H) thin film light emitting diode | 47 |
| 6.7 | Picture of the a-SiC:H thin film light emitting diodes fabricated on a glass substrate | 47 |

LIST OF FIGURES (continued)

Figures

| | | |
|------|---|----|
| 6.8 | I(V) curves of a-SiC:H TFLEDs having different optical energy gaps of the i-layers | 48 |
| 6.9 | Room temperature electroluminescent spectra of a-SiC:H TFLEDs. The parameter is the optical energy gap of the i-layer | 49 |
| 6.11 | Relationship between the photocurrent output of the a-SiGe:H TFPD and the injection current density of a-SiC:H TFLED constructed in the amorphous photocoupler type (a) | 51 |
| 6.12 | Relationship between the photocurrent output and applied voltage of a-SiGe:H photoresistor which is illuminated by the light from a-SiC:H TFLED | 52 |

Appendix

| | | |
|---|---|----|
| 1 | Structure of a-SiGe:H thin film solar cell | 63 |
| 2 | Photograph of the example of a-SiGe:H thin film solar cells | 64 |
| 3 | Configuration of the measurement system of the conversion efficiency of solar simulator | 65 |

LIST OF TABLES

| Tables | Page |
|--|------|
| 2.1 The summary of the glow discharge plasma CVD system | 6 |
| 2.2 Materials of substrates and the objectives | 8 |
| 2.3 Typical preparation conditions of the a-SiGe:H by glow discharge plasma CVD method | 10 |
| 3.1 Typical preparation conditions for undoped a-SiGe:H | 11 |
| 4.1 Preparation conditions for undoped a-SiGe:H having substrate temperature as a parameter | 24 |
| 4.2 Preparation conditions for undoped a-SiGe:H | 26 |
| 5.1 Preparation conditions of p-i-n layers by the glow discharge plasma CVD method | 33 |
| 6.1 Examples of applications of photocouplers | 40 |
| 6.2 Fabrication conditions of a-SiC:H p-i-n junction thin film LEDs (TFLEDs) by glow discharge plasma CVD | 46 |
| 6.3 Preparation conditions of undoped a-SiGe:H films | 50 |
| Appendix | |
| 1 Preparation conditions of a-SiGe:H thin film solar cells by the glow discharge plasma CVD | 63 |

CHAPTER 1

Introduction

1.1 Background

An amorphous photocoupler is a functional device, which transfers an electrical signal to an optical signal and also transfers the optical signal back to an electrical signal. The applications of the device are for example, interfaces for signal transmission, position and size detectors of moving objects, tape end detectors, etc. It has been reported that amorphous photocouplers consisting of a hydrogenated amorphous silicon carbide p-i-n thin film light emitting diode (a-SiC:H TFLED) and a hydrogenated amorphous silicon p-i-n thin film photodiode (a-Si:H TFPD) has been fabricated [1]. So far the amorphous TFPD was made of a-Si:H, therefore it was mostly sensitive to the visible light. For this reason, the a-SiC:H TFLED had to contain the i-a-SiC:H layer which had a large optical energy gap of more than 2.8 eV so that it could emit visible light (orange to white blue). However, the a-SiC:H TFLED which possessed such a large optical energy gap needed to be operated by a high voltage of 20-25 V.

A possible solution for decreasing the operating voltage of the TFLED is to reduce the optical energy gap of the i-a-SiC:H layer to about 2.2-2.5 eV. The i-a-SiC:H having an optical energy gap in this range emits the light from red to near infrared region [1]. At the same time the optical energy gap of the intrinsic layer in the TFPD has to be decreased to about 1.4 - 1.5 eV, and this can be done by using hydrogenated amorphous silicon germanium (a-SiGe:H) material as the intrinsic layer in the TFPD.

Hydrogenated amorphous silicon germanium alloy has attracted much attention due to its narrow optical energy gap which performs a better photoresponse at longer wavelength as compared to hydrogenated amorphous silicon (a-Si:H).

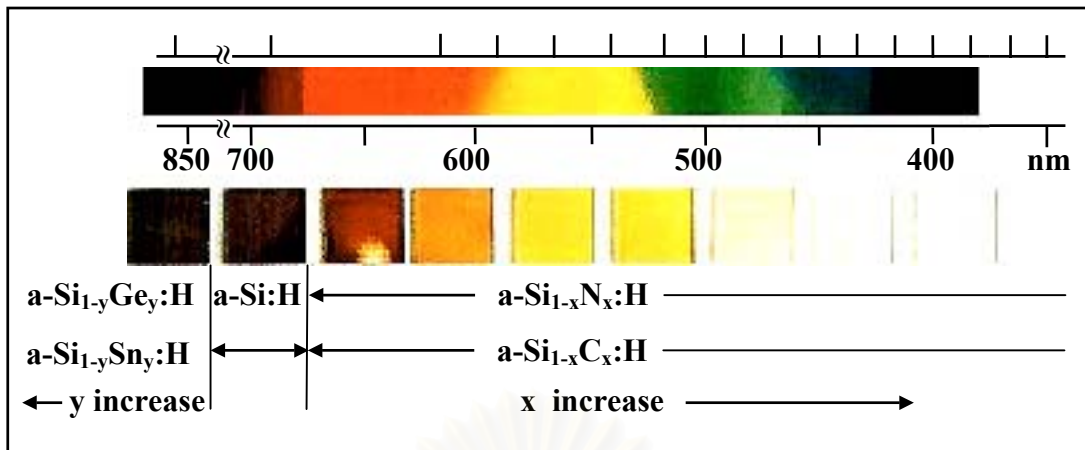


Figure 1.1 Picture of a-Si:H and other amorphous silicon alloys deposited on glass substrates.

Figure 1.1 shows the colors of a-Si:H thin films and other amorphous silicon alloys deposited on glass substrates. The colors of the films change as the optical energy gaps of the films change. It is expected that a-SiGe:H responds to the infrared light, due to its narrow optical energy gap.

It has been reported that a-SiGe:H can be prepared by the glow discharge plasma CVD method from the gas mixture of GeH_4 and SiH_4 [2-6]. The optical energy gap of a-SiGe:H can be reduced from 1.8 eV to 1.1 eV by increasing the gas flow rate ratio of $\text{GeH}_4/(\text{GeH}_4+\text{SiH}_4)$ [7]. So far there have been several reports on the applications of a-SiGe:H as an active layer in amorphous silicon solar cell. However, there has been no report on the application of a-SiGe:H as an active layer in amorphous photodiode. In this thesis, the report will be done on the preparation technology of high photo-conductivity a-SiGe:H and the application of the high photo-conductivity a-SiGe:H as an active layer in infrared light photodiode as well as photoresistor. The presentation will also be done on the application of the a-SiGe:H thin film photodiode as the infrared light detector in the amorphous photocoupler.

1.2 Objectives

- 1) Prepare undoped a-SiGe:H by the glow discharge plasma CVD method from the gas mixture of GeH₄, SiH₄ and H₂.
- 2) Study the basic properties, including structural-, optical- and electrical-properties of undoped a-SiGe:H.
- 3) Study the preparation technologies for obtaining high photo-conductivity a-SiGe:H having the optical energy gap of 1.4-1.6 eV. The focus will be paid on the substrate temperature and hydrogen gas dilution.
- 4) Fabricate infrared light a-SiGe:H thin film photodiode and photoresistor, and measure their basic output characteristics.
- 5) Fabricate infrared light amorphous photocoupler consisting of a-SiC:H thin film light emitting diode and a-SiGe:H thin film photodiode and thin film photoresistor, and measure the basic characteristics of the photocouplers.

1.3 Structure of the Thesis

The thesis consists of seven chapters and an annex.

In chapter 1, a brief background and objectives of the work are described.

In chapter 2, the description is done on the preparation processes of undoped a-SiGe:H by the glow discharge plasma CVD method. The configuration of the glow discharge plasma CVD is presented. The substrate preparation and film deposition processes are described.

In chapter 3, the results of the study of the basic properties of undoped a-SiGe:H is presented. The basic properties includes the structural- (IR, ESR), optical- (absorption, optical energy gap), and electrical- (dark and photo-conductivities) properties. The relation between the optical energy gaps of a-SiGe:H and conductivities is discussed.

In chapter 4, the technologies of improvement of photo-conductivity of a-SiGe:H is described. It is showed that the substrate temperature and hydrogen gas dilution are important preparation parameters.

In chapter 5, the structure and fabrication of infrared light a-SiGe:H thin film photodiode are mentioned. The output characteristics of the a-SiGe:H photodiode are presented.

In chapter 6, the structure and fabrication of amorphous photocouplers consisting of a-SiC:H thin film light emitting diode and a-SiGe:H photodiode and photoresistor are described. The basic characteristics of the amorphous photocouplers are presented and discussed.

In chapter 7, the conclusions of the work are given.

In an annex, some results of the preliminary experiment on the fabrication of a-SiGe:H thin film solar cell are briefed.



สถาบันวิทยบริการ
จุฬาลงกรณ์มหาวิทยาลัย

CHAPTER 2

Preparation of Hydrogenated Amorphous Silicon Germanium by Glow Discharge Plasma CVD Method

2.1 Introduction

The purpose of this work is to fabricate an amorphous thin film photocoupler which operates in the infrared light range. Therefore, the photodiode which is the detector must contain the small optical energy gap of the intrinsic layer, for example, lower than 1.7 eV. It has been widely reported that a-SiGe:H can serve this requirement [7]. This material can be prepared by several methods, such as sputtering, thermal CVD and glow discharge plasma CVD.

The glow discharge plasma CVD is the most popular deposition method for the preparation of amorphous silicon alloys [8]. There are several advantage features in the glow discharge plasma CVD method, e.g. easy technology, low temperature process, low cost, possibility of using inexpensive substrates of almost size or shape, providing good quality of films [9]. The film deposited by the glow discharge plasma CVD method always contains several percentages of hydrogen atoms which act as the terminators of dangling bonds.

In this chapter, the structure of the glow discharge plasma CVD system is presented. The preparation of substrates for a-SiGe:H thin film deposition and the deposition process are described in details.

2.2 Preparation of a-SiGe:H by Glow Discharge Plasma CVD System

2.2.1 Structure of Glow Discharge Plasma CVD System

The glow discharge plasma CVD system employed in this work is the conventional radio frequency (RF) glow discharge system. The system consists of two parts; the CVD part and the gas control part.

The frequency of the RF power source is 13.56 MHz. The matching box is used for transferring the maximum electrical power to the load, i.e. plasma. The gas control part consists of pressure regulators, filters, valves, flow meters and source gases. The source gases in the system are SiH₄, B₂H₆, PH₃, GeH₄, CH₄, C₂H₄, H₂ and N₂. The

flow rates of gases are controlled by the needle valves and flow meters. The pressure in the reaction chamber is pumped down to the background pressure (0.01 Torr) by a rotary pump. The diameter of the RF electrode is 10 cm. The distance between the RF electrode and the ground electrode is fixed at 2.5 cm. The substrate temperature is controlled by the heater under the susceptor. The maximum temperature of the heater in this system is 400°C. Table 2.1 summarizes details of the glow discharge plasma CVD system. Figure 2.1 shows a schematic diagram of the glow discharge plasma CVD system.

Table 2.1 Summary of the glow discharge plasma CVD system.

| | |
|-------------------------------|---|
| Chamber | Diameter 22 cm, Pyrex glass |
| Susceptor | Diameter 10 cm |
| Maximum temperature of heater | 400 °C |
| Electrode | Capacitive coupling |
| RF power | 13.56 MHz, maximum 150 W |
| Pressure | 0.01 – 10 Torr |
| Gas dilution | SiH ₄ /H ₂ = 10% |
| | GeH ₄ /H ₂ = 10% |
| | CH ₄ /H ₂ = 10% |
| | C ₂ H ₄ /H ₂ = 10% |
| | B ₂ H ₆ /H ₂ = 500 ppm |
| | PH ₃ /H ₂ = 500 ppm |

สถาบันวิทยบริการ
จุฬาลงกรณ์มหาวิทยาลัย

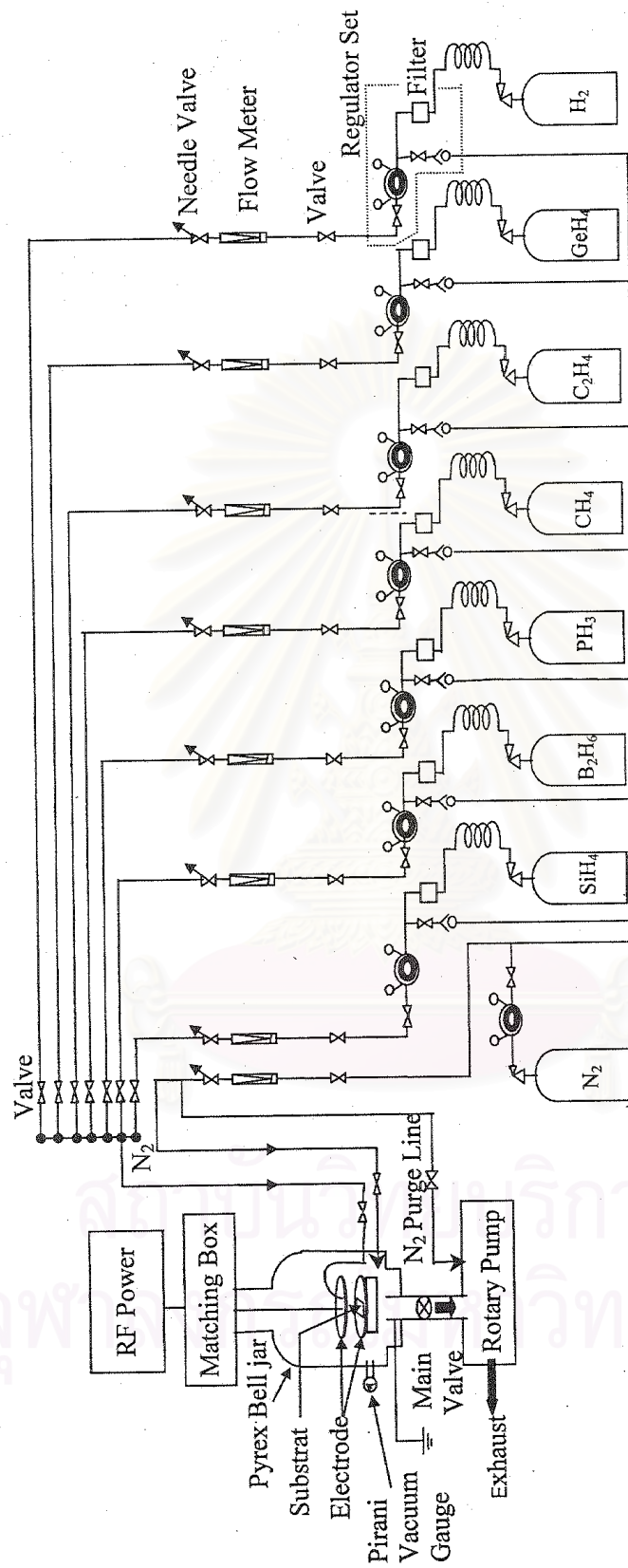


Figure 2.1 Schematic diagram of the glow discharge plasma CVD system.

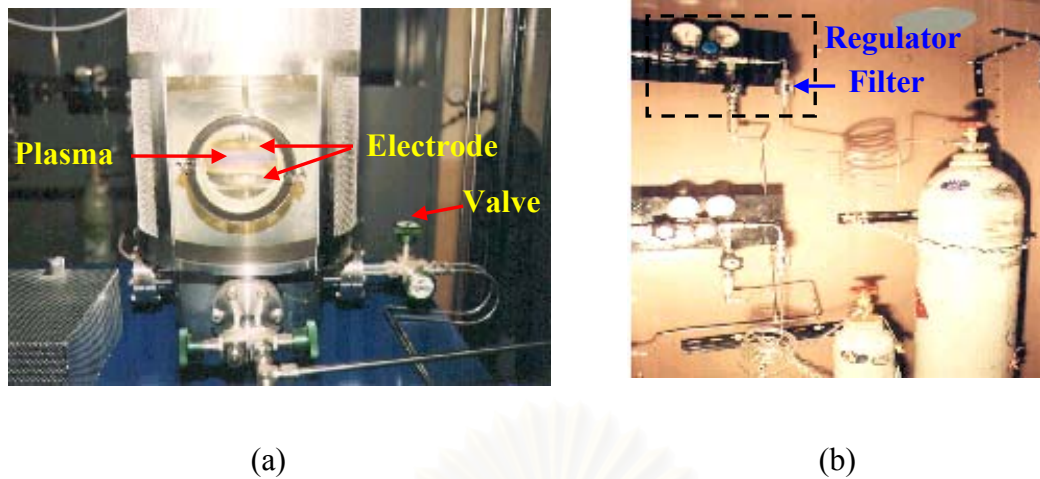


Figure 2.2 Photographs of the glow discharge plasma CVD system at the Semiconductor Device Research Laboratory, Chulalongkorn University. (a) reaction chamber and (b) a part of the gas system.

2.2.2 Preparation of Substrates

In order to study the basic properties of the a-SiGe:H films, a-SiGe:H thin films were deposited on various kinds of substrates by the glow discharge plasma CVD method. Table 2.2 summarizes the materials of the substrates and the objectives.

Table 2.2 Materials of substrates and objectives.

| Substrate | Objective |
|--|---|
| · Corning glass No. 7059 (2 cm × 2 cm × 1 mm) | · Optical absorption coefficient (α) · Electrical conductivity (σ) |
| · Single crystalline silicon wafer with high resistivity (mirror surface 1 cm × 1 cm × 0.5 mm) | · Infrared light absorption |
| · Micro slide glass (2 cm × 2 cm × 1 mm) | · Spin density (Dangling bond density) measured by Electron Spin Resonance (ESR) |

The substrates were cleaned by the processes as follows:

- Trichloroethylene Ultrasound 20 minutes
- Acetone Ultrasound 20 minutes
- Methylalcohol Ultrasound 20 minutes.

In the case of single crystalline Si wafer, after the Si wafer was cleaned by the processes described above, the oxide layer on the surface was etched by hydrofluoric acid diluted in water (HF: H₂O = 1:10) about 10 minutes and then rinsed by de-ionized (DI) water.

2.2.3 Deposition of a-SiGe:H

The deposition process of a-SiGe:H by the glow discharge plasma CVD is shown in Figure 2.2

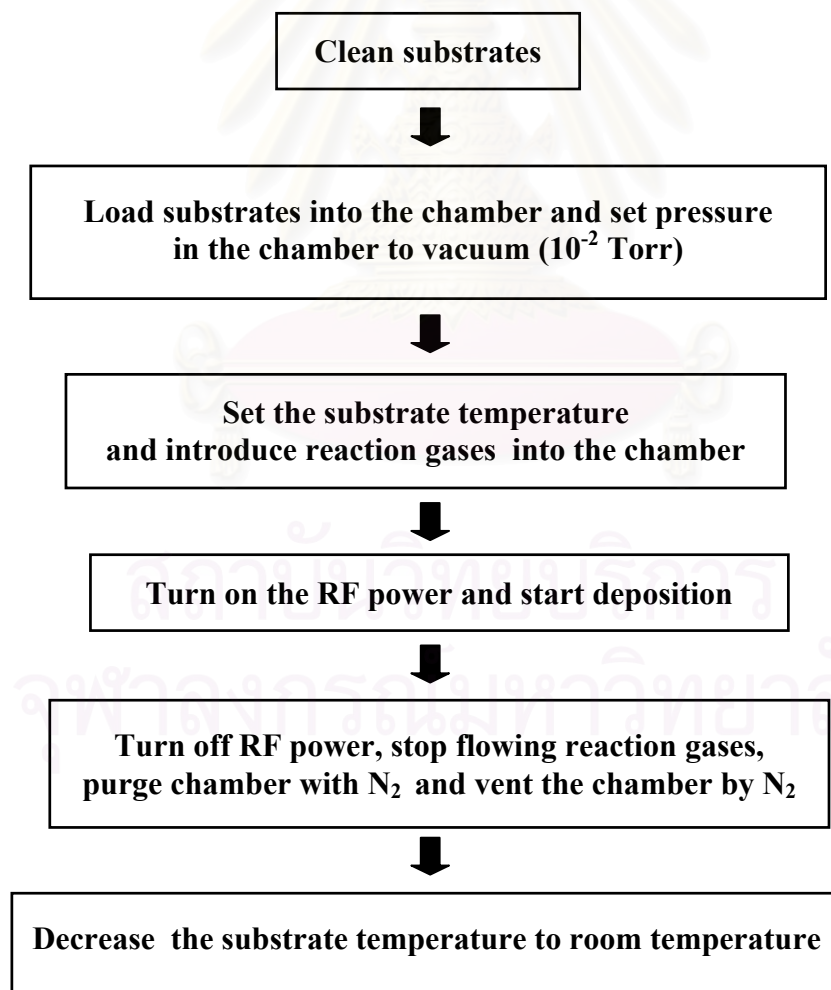


Figure 2.3 Deposition process of a-SiGe:H by the glow discharge plasma CVD.

The a-SiGe:H thin films were deposited by using GeH₄ and SiH₄ as the active gases and H₂ as the diluent. The substrate temperature was changed from 190°C to 350 °C. The total gases pressure during the deposition were 1.0-10 Torr according to the preparation conditions. All of a-SiGe:H films were deposited for 90 minutes and the thicknesses of the films were 0.5-0.8 μm. Table 2.2 shows the typical preparation conditions of the a-SiGe:H by the glow discharge plasma CVD method.

Table 2.3 Typical preparation conditions of the a-SiGe:H by glow discharge plasma CVD method.

| | |
|-----------------------|--|
| Power Source | C-Coupling, 13.56 MHz |
| RF Power | 3 W |
| Substrate Temperature | 190°C - 350°C |
| Reaction Gases | SiH ₄ + GeH ₄ + H ₂ |
| Background Pressure | 0.01 Torr |

Summary

1. The a-SiGe:H thin films were deposited by the glow discharge plasma CVD method using SiH₄, GeH₄ as the active gases and H₂ as the diluent.
2. The a-SiGe:H thin films were deposited on various kinds of substrates, i.e. corning glass No. 7059, single crystalline silicon wafers and micro slide glasses in order to study the basic properties, i.e. structural, optical and electrical properties.
3. The results of the basic properties are described in the next chapter.

จุฬาลงกรณ์มหาวิทยาลัย

CHAPTER 3

Basic Properties of Undoped a-SiGe:H

3.1 Introduction

In this chapter, undoped a-SiGe:H thin films deposited on various kinds of substrates including of single crystalline silicon wafers, micro slide glasses and corning glasses No.7059 were used to investigate the basic properties of a-SiGe:H thin films; i.e. the structural, optical and electrical properties, respectively by several kinds of methods.

The structural properties of a-SiGe:H films were investigated by Electron Spin Resonance (ESR) which provided the dangling bond density in the films. The measurement of infrared light (IR) absorption gave the Ge contents in the films. The optical properties were studied by using spectra of the optical absorption coefficients and the optical energy gaps calculated from Tauc's plots. The electrical properties included the photo-conductivity (σ_{ph}), dark-conductivity (σ_D) and the ratio of the photo-conductivity to the dark-conductivity (σ_{ph}/σ_D).

The preparation conditions of undoped a-SiGeH thin films used for investigating the basic properties were summarized in Table 3.1

Table3.1 Preparation conditions for undoped a-SiGe:H.

| | |
|--------------------------------|--------------------|
| RF power | 3 watt (13.56 MHz) |
| Substrate temperature | 190°C |
| Deposition pressure | 1.0-1.5 Torr |
| SiH ₄ gas flow rate | 10-50 sccm |
| GeH ₄ gas flow rate | 10-50 sccm |
| H ₂ gas flow rate | 20 sccm |

3.2 Structural properties of a-SiGe:H

3.2.1 Measurement of Germanium Contents in a-SiGe:H by Infrared Transmittance Spectra

Germanium contents in a-SiGe:H were evaluated by using the infrared transmittance spectrum technique taken by the PERKIN ELMER model 1760X FT-IR spectrometer. The single crystalline Si wafer with high resistivity was used as the substrate. The substrate size was $1.0 \times 1.0 \text{ cm}^2$.

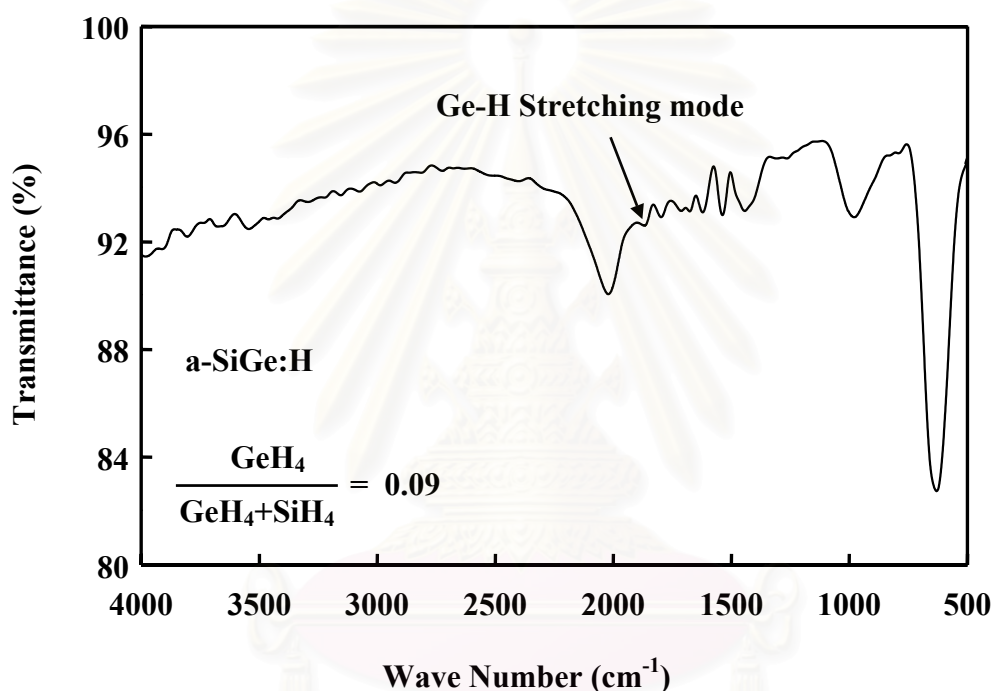


Figure 3.1 An example of infrared transmittance spectrum for an a-SiGe:H film prepared at the gas flow rate ratio $x = \text{GeH}_4 / (\text{GeH}_4 + \text{SiH}_4) = 0.09$.

Figure 3.1 shows an example of the infrared transmittance spectrum measured at room temperature for undoped a-SiGe:H thin film prepared at the gas flow rate ratio $x = \text{GeH}_4 / (\text{GeH}_4 + \text{SiH}_4) = 0.09$. The absorption peak of Ge-H vibration was observed around $1,850\text{-}1,900 \text{ cm}^{-1}$. The absorption coefficients of Ge-H were calculated from the transmittance coefficients as follows.

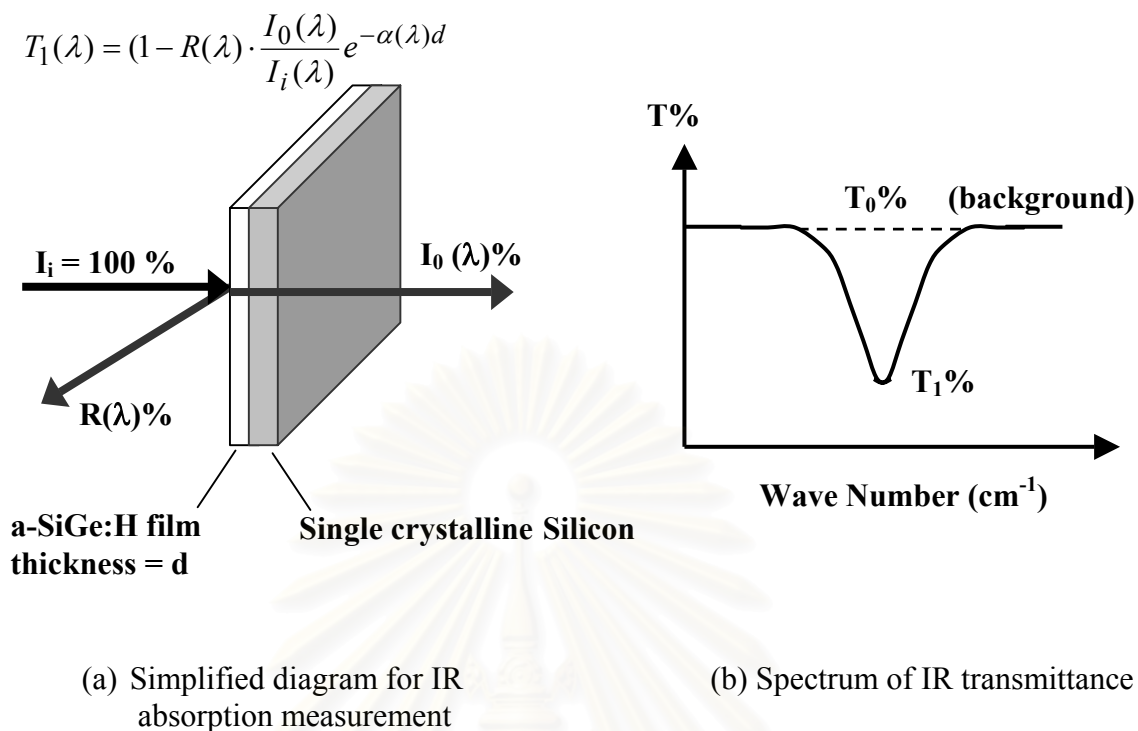


Figure 3.2 The calculation of IR absorption coefficient of a-SiGe:H from the spectrum of IR transmittance.

Figure 3.2 (a) shows an a-SiGe:H thin film with thickness d having absorption coefficient $= \alpha(\lambda)$ and reflective coefficient $= R(\lambda)$. Assuming that most of the reflection occurs at the surface of a-SiGe:H thin film, the transmittance $T(\lambda)\%$ can be written as follow:

$$T_1(\lambda) = (1 - R(\lambda)) \cdot \frac{I_0(\lambda)}{I_i(\lambda)} e^{-\alpha(\lambda)d} \quad (3.1)$$

Given the transmittance at the background $= T_0(\lambda)\%$, so that

$$T_0(\lambda) = (1 - R(\lambda)) \cdot \frac{I_0}{I_i} \quad (3.2)$$

Divide eq. (3.1) by eq. (3.2), it can be shown that

$$\frac{T_1(\lambda)}{T_0(\lambda)} = e^{-\alpha(\lambda)d} \quad (3.3)$$

Therefore,

$$\alpha(\lambda) = \frac{1}{d} \ln \left[\frac{T_0(\lambda)}{T_1(\lambda)} \right] \quad (3.4)$$

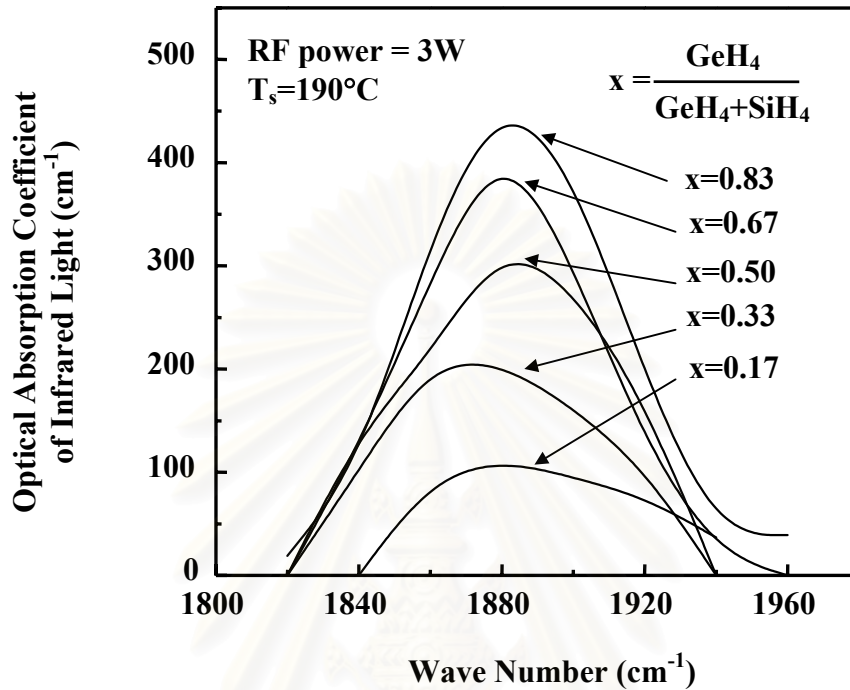


Figure 3.3 Infrared absorption coefficient spectra of Ge-H atoms of a-SiGe:H (stretching mode).

Figure 3.3 shows results of the measurement of the IR absorption coefficients of a-SiGe:H thin films. x denotes gas flow rate ratio of $\text{GeH}_4/(\text{GeH}_4+\text{SiH}_4)$. It shows that the amount of the Ge-H atoms increase as the gas flow rate of GeH_4 increases. This implies that the Ge contents in a-SiGe:H thin films can be changed by varying the gas flow rate of GeH_4 .

3.2.2 Measurement of Dangling Bond Density in a-SiGe:H Films by Electron Spin Resonance (ESR)

Electron Spin Resonance (ESR) is a useful technique for obtaining the information about defects in amorphous semiconductors. In this work, ESR spectra were taken by the Joel model JES-RE2X ESR spectrometer. Normal covalent bonds have two electrons with opposite spins and therefore zero net spin. A dangling bond of a-SiGe:H has a single electron with unpaired spin and will be split by a magnetic

field. ESR are the result of the transitions of the lone-paired spin between the split energy levels. The transition efficiently occurs when electromagnetic wave (microwave frequency) is applied. The strength of the microwave absorption gives the density of the lone-paired electrons and the ESR spectrum gives information about local bonding structures. The technique is sensitive, being able to detect about 10^{11} spins and well suited for the measurement of low defect densities [10]. The purpose of this measurement is to study the structural properties and the film quality of undoped a-SiGe:H films.

Figure 3.4 shows the relationship between ESR spin density and gas flow rate ratio $x = \text{GeH}_4/(\text{GeH}_4+\text{SiH}_4)$. The thickness of a-SiGe:H films is around $0.5 \mu\text{m}$. It shows that when x increases from 0.17 to 0.67, the dangling bond density increased from $2 \times 10^{17} \text{cm}^{-3}$ to $3 \times 10^{18} \text{cm}^{-3}$. This means that when the Ge contents increase the dangling bond density in the film increases.

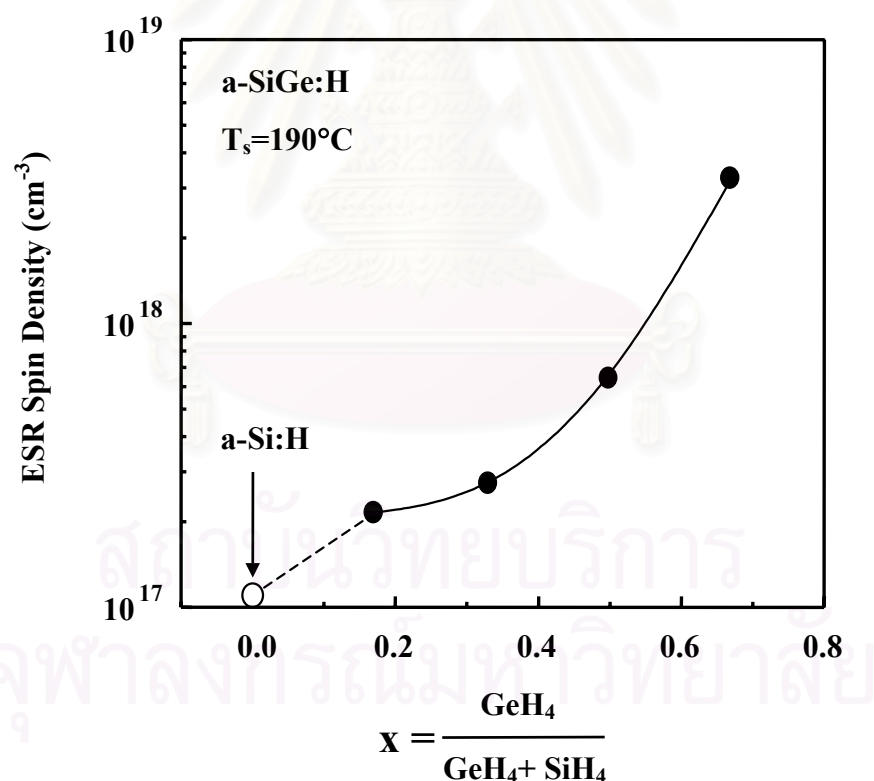


Figure 3.4 Relationship between ESR spin density and gas flow rate ratio for a-SiGe:H.

3.3 Optical Properties of a-SiGe:H

An amorphous silicon-based thin film photodiode which is sensitive to infrared light should have the optical energy gap (E_{opt}) of the intrinsic layer less than 1.7 eV. The a-SiGe:H is an interesting material since the optical energy gap can be changed from 1.1-1.85 eV by varying Ge contents in the film [7]. Figure 3.5 shows the optical absorption coefficient spectra of a-SiGe:H prepared in the work. It is seen that the spectra move to the lower photon energy as the gas flow rate ratio x increases. The optical energy gaps of a-SiGe:H can be determined by the well-known Tauc's plots ($\sqrt{ah\nu}$ vs $h\nu$). Figure 3.6 shows the Tauc's plots for various a-SiGe:H. The interception of a straight line on the x-axis represents the optical energy gap of an a-SiGe:H.

Figure 3.7 summarizes the optical energy gap of a-SiGe:H prepared with different gas flow rate x . It is found that as x increases from 0.09 to 0.83, the optical energy gap of a-SiGe:H decreases from 1.7 to 1.14 eV and the colors of the films change from dark brown to dark gray.

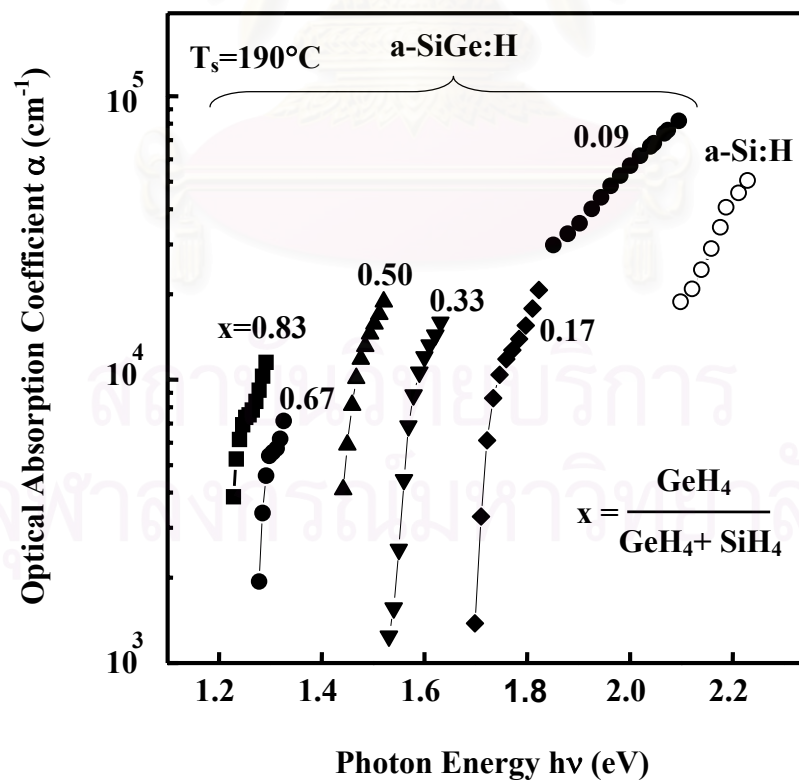


Figure 3.5 The optical absorption coefficient spectra near the fundamental band edge of a-SiGe:H. The parameter (x) is the $\text{GeH}_4/\text{GeH}_4+\text{SiH}_4$ gas flow ratio.

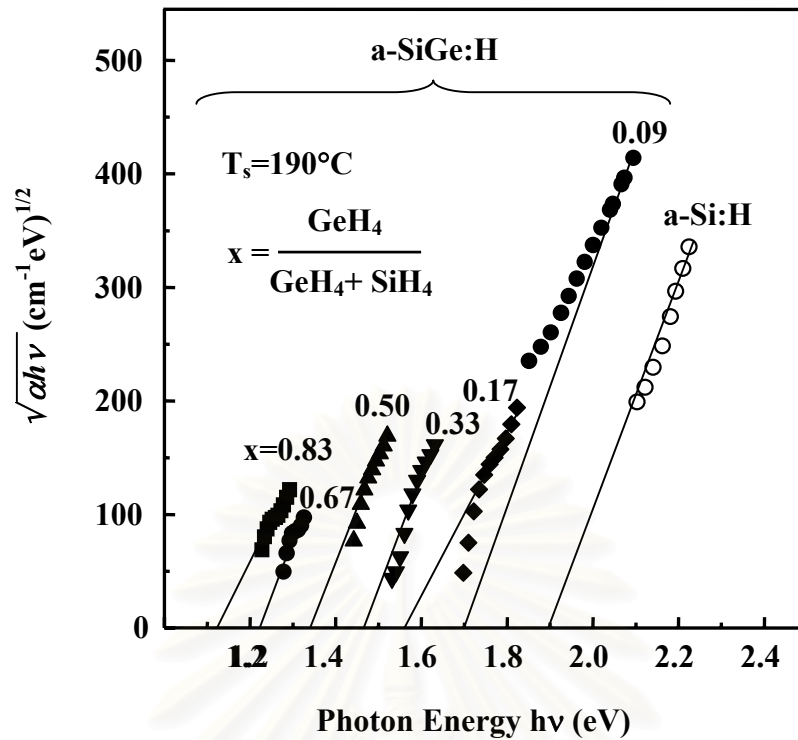


Figure 3.6 Tauc's plot for the determination of the optical energy gap of a-SiGe:H.

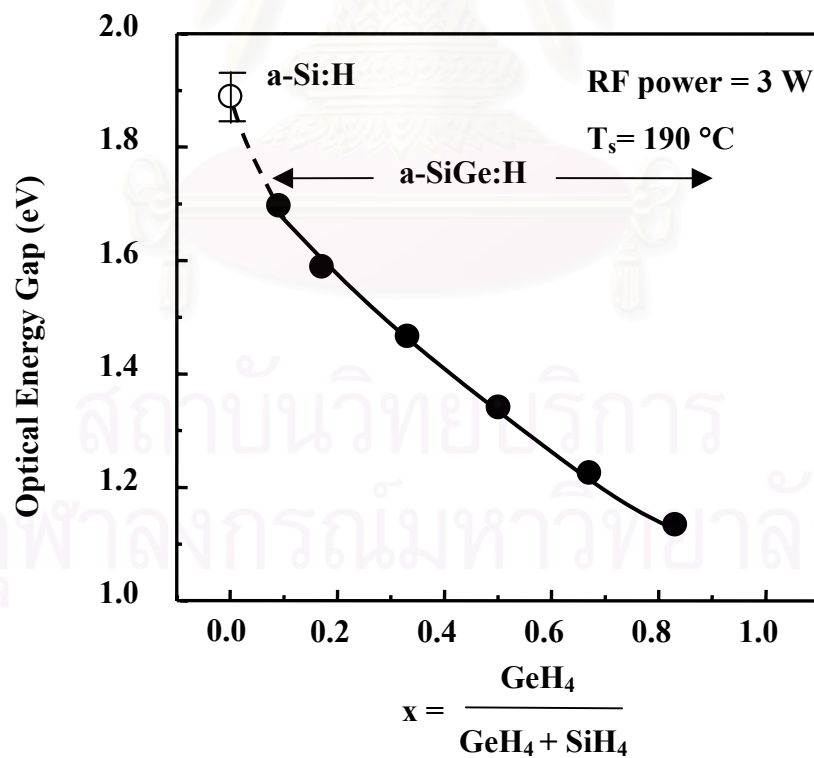


Figure 3.7 Relationship between the gas flow rate ratio x and the optical energy gap of undoped a-SiGe:H.

3.4 Electrical Properties of a-SiGe:H

In this section, the results of the study on the electrical properties (photo-conductivity and dark conductivity) of undoped a-SiGe:H is described. The photoconductivity was measured by using the solar simulator (KATOS LPS 255 HR) as a light source having the intensity of 100 mW/cm^2 (AM1). Figures 3.8 (a) and (b) shows the schematic diagrams of the measurement systems of the dark- and photo-conductivities, respectively, for a-SiGe:H in the work. Two-co-planar Al electrodes were deposited on the surface of the a-SiGe:H. The size of each electrode was $1 \text{ mm} \times 1.5 \text{ cm}$ and the distance between the electrodes was 1 mm. The pico-ampere meter and voltage source was the model HP 4140B. The voltage applied to the co-planar electrodes was 10 V. Using a simple calculation, the conductivity is calculated as follows:

$$\sigma = \frac{w \times I}{l \times d \times V} \quad (\text{S/cm}) \quad (3.5)$$

where σ is the conductivity,

w is the distance between electrodes (1mm),

l is the length of the electrodes (15 mm),

d is the thickness of a-SiGe:H (0.5-1.0 μm),

I is the output current,

V is the applied voltage.

สถาบันวิทยบริการ
จุฬาลงกรณ์มหาวิทยาลัย

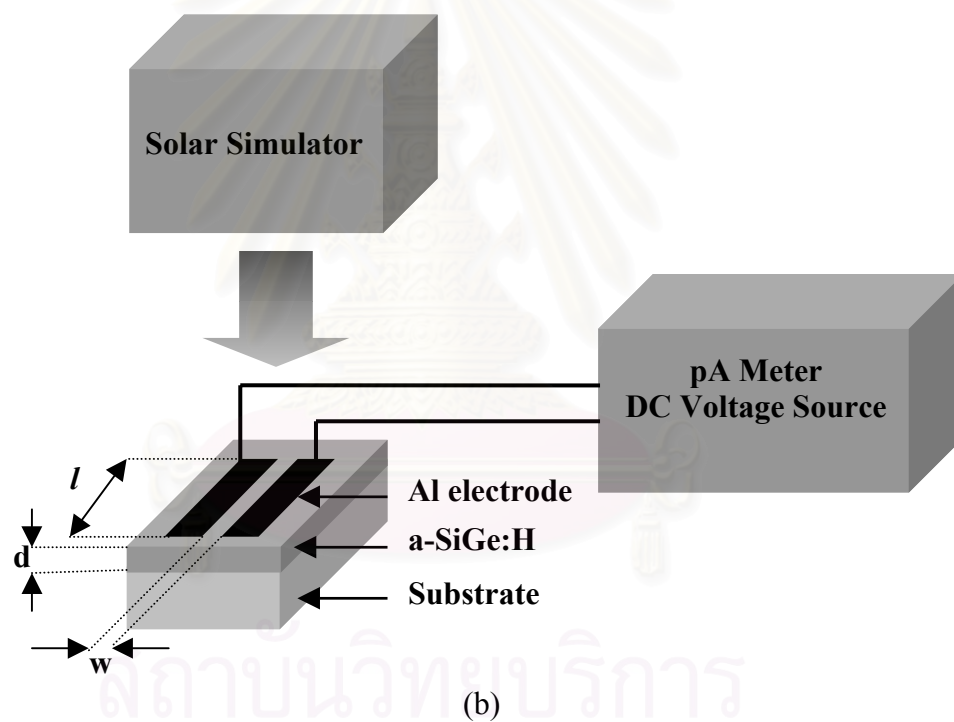
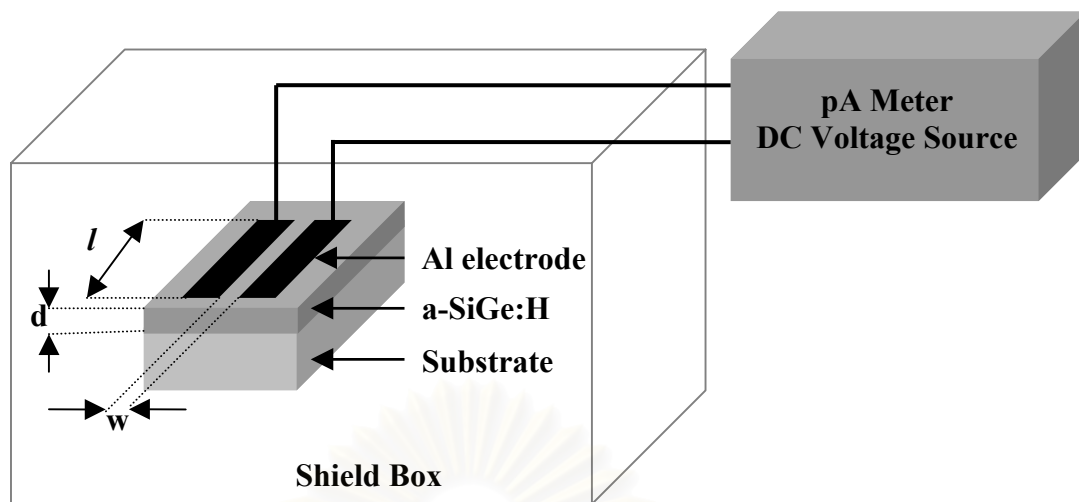


Figure 3.8 Schematic diagrams of the measurements of (a) dark-conductivity and (b) photo-conductivity for a-SiGe:H.

In this work, a study has been done on the relationship between the conductivity and the gas flow rate ratio of $\text{GeH}_4/(\text{GeH}_4+\text{SiH}_4)$. Figure 3.9 shows the relationship between the dark-conductivity (σ_D), the photo-conductivity (σ_{ph}) as well as the ratio of σ_{ph}/σ_D for a-SiGe:H prepared by different gas flow rate ratio. It is seen that the dark-conductivity increases from 10^{-10} to 10^{-4} S/cm as the gas flow rate ratio increases from 0.17 to 0.83. The increase of the dark-conductivity with Ge contents, is due to the decrease of the optical energy gap of a-SiGe:H and the shift of Fermi level towards the conduction band.

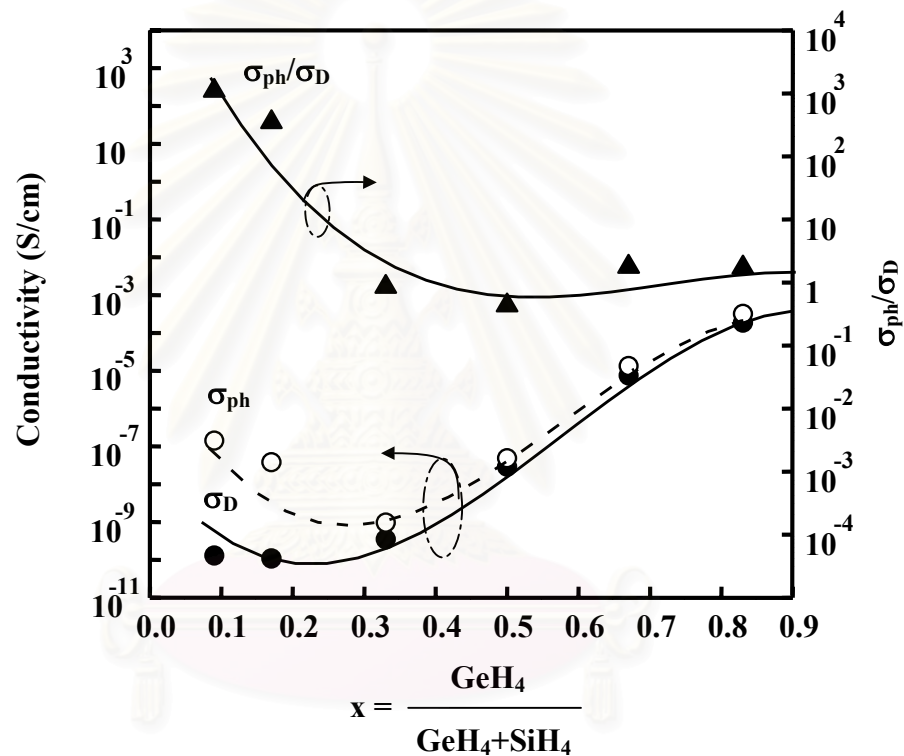


Figure 3.9 Relationship between dark-conductivity (σ_D), photo-conductivity (σ_{ph}) and the ratio of σ_{ph}/σ_D for a-SiGe:H prepared by different gas flow rate ratio ($\text{GeH}_4/(\text{GeH}_4+\text{SiH}_4)$).

The ratio of σ_{ph}/σ_D is in the order of 10^3 only when the ratio of $\text{GeH}_4/(\text{GeH}_4+\text{SiH}_4)$ is as small as 0.09. The ratio of σ_{ph}/σ_D drastically decreases to less than 10 when the ratio of $\text{GeH}_4/(\text{GeH}_4+\text{SiH}_4)$ is greater than about 0.5. The large decrease of the σ_{ph}/σ_D with increasing $\text{GeH}_4/(\text{GeH}_4+\text{SiH}_4)$ is considered to be due to the large increase of the dangling bond density in a-SiGe:H [11].

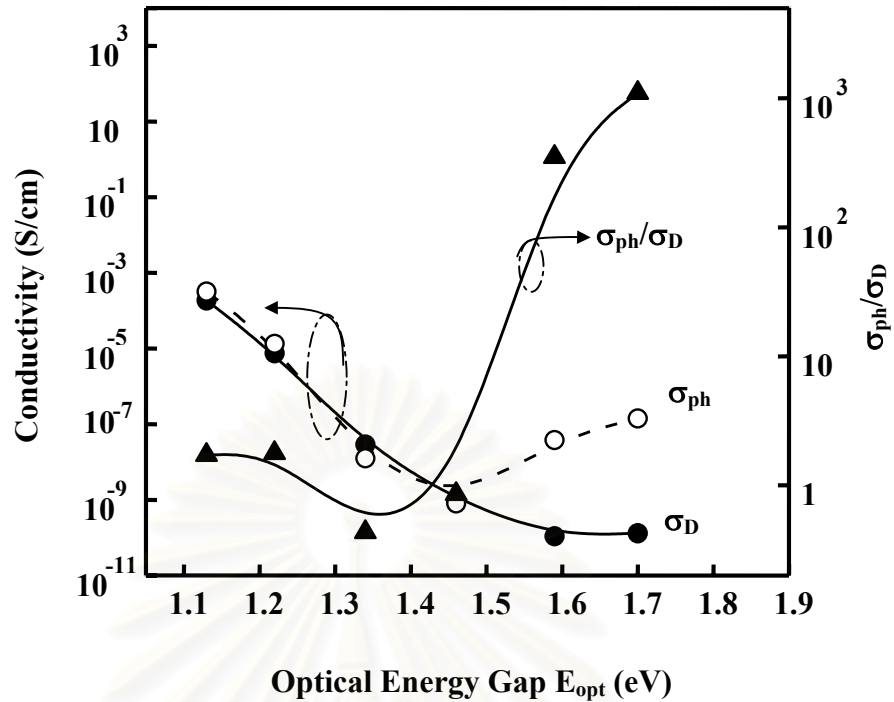


Figure 3.10 Relationship between the conductivities and the optical energy gaps for undoped a-SiGe:H.

Figure 3.10 summarizes the relationship between the conductivities and the optical energy gaps for undoped a-SiGe:H. It is again clearly seen that the ratio of σ_{ph}/σ_D decreases as the optical energy gap of undoped a-SiGe:H decreases.

In order to apply the a-SiGe:H as an active layer in a photodiode or a solar cell, it is necessary to improve the photo-conductivity of the a-SiGe:H. In this work, several attempts to improve the photo-conductivity of a-SiGe:H have been done. The details of the improvement technologies of the photo-conductivity of a-SiGe:H will be presented in details in chapter 4.

Summary

The basic properties including structural, optical and electrical properties of undoped a-SiGe:H have been studied. The results can be summarized as follows:

1. The a-SiGe:H can be prepared by the gas mixture of $\text{GeH}_4 + \text{SiH}_4$ by the glow discharge plasma CVD method.
2. According to the results of the infrared absorption spectra, there are several atomic bonding in the films, for examples, Si-H_x, Ge-H_y, Si-Ge, etc. The increase of Ge contents can be achieved by increasing the gas flow rate ratio of $\text{GeH}_4 / (\text{GeH}_4 + \text{SiH}_4)$.
3. The optical energy gap of a-SiGe:H decreases from about 1.7 eV to about 1.1 eV as the ratio of $x = \text{GeH}_4 / (\text{GeH}_4 + \text{SiH}_4)$ increases from about 0.09 to about 0.83. These results show that the optical energy gaps of a-SiGe:H can be widely changed by adjusting the ratio of x.
4. The result of measurement of ESR shows that the dangling bond density in a-SiGe:H increases as the gas flow rate ratio $x = \text{GeH}_4 / (\text{GeH}_4 + \text{SiH}_4)$ increases (also as the Ge contents increase).
5. The dark-conductivity of undoped a-SiGe:H increases from 10^{-10} to 10^{-4} S/cm as the gas flow rate ratio $x = \text{GeH}_4 / (\text{GeH}_4 + \text{SiH}_4)$ increases from 0.17 to 0.83. The increase of the dark-conductivity with Ge contents, is due to the decrease of the optical energy gap of a-SiGe:H and the shift of Fermi level towards the conduction band.
6. The ratio of $\sigma_{\text{ph}} / \sigma_{\text{D}}$ is in the order of 10^3 only when the ratio of $\text{GeH}_4 / (\text{GeH}_4 + \text{SiH}_4)$ is as small as 0.09. The ratio of $\sigma_{\text{ph}} / \sigma_{\text{D}}$ drastically decreases to less than 10 when the ratio of $\text{GeH}_4 / (\text{GeH}_4 + \text{SiH}_4)$ is greater than about 0.5.
7. The large decrease of the $\sigma_{\text{ph}} / \sigma_{\text{D}}$ with increasing $\text{GeH}_4 / (\text{GeH}_4 + \text{SiH}_4)$ is considered to be due to the large increase of the dangling bond density in a-SiGe:H.
8. In order to apply the a-SiGe:H as an active layer in a photodiode or a solar cell, it is necessary to improve the photo-conductivity of the a-SiGe:H as will be presented in details in chapter 4.

CHAPTER 4

Improvement of Optoelectronic Properties of a-SiGe:H

4.1 Introduction

In order to apply a-SiGe:H as an active layer in a p-i-n junction amorphous thin film photodiode and a solar cell which are sensitive to infrared light, the optical energy gap of a-SiGe:H should be small and the photo-conductivity of the a-SiGe:H should be as high as possible. However, according to the results in chapter 3, it was found that the photo-conductivity drastically decreases several order of magnitude as the optical energy of a-SiGe:H decreases from 1.7 eV to 1.1 eV.

In this chapter, a series of attempts to improve the optoelectronic properties, especially the photo-conductivity of undoped a-SiGe:H are described. The first attempt was done by the optimization of the substrate temperature during growing films. The second attempt was done by the optimization of the gas flow rate ratio of H₂ to (GeH₄+SiH₄). According to these trials, the photo-conductivity of undoped a-SiGe:H has been improved by several order of magnitude.

4.2 Improvement of Photo-Conductivity of a-SiGe:H by Optimization of Substrate Temperature

It has been found for a long time that substrate temperature is one of the most important preparation conditions for hydrogenated amorphous silicon based alloys, including a-Si:H, a-SiC:H and a-SiGe:H [5,12,14]. In chapter 3, the substrate temperature for the preparation of undoped a-SiGe:H was fixed at 190 °C. Therefore, in this section, the effect of the substrate temperature on the photo-conductivity of a-SiGe:H has been investigated. In the experiments, the substrate temperature was changed from 190 °C to 350 °C. Table 4.1 summarizes the preparation conditions for undoped a-SiGe:H having substrate temperature as a parameter.

Table 4.1 Preparation conditions for undoped a-SiGe:H having substrate temperature as a parameter.

| | |
|--------------------------------|--------------------|
| RF power | 3 watt (13.56 MHz) |
| Substrate temperature | 190-350°C |
| SiH ₄ gas flow rate | 50 sccm |
| GeH ₄ gas flow rate | 5 sccm |
| H ₂ gas flow rate | 100 sccm |

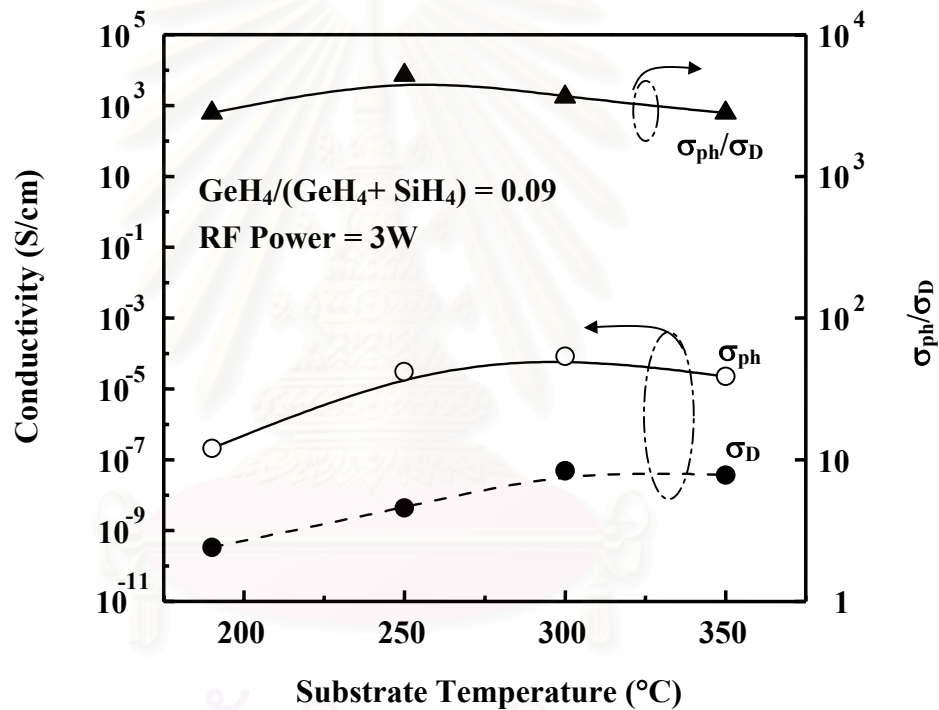


Figure 4.1 Relationship between conductivity of a-SiGe:H and substrate temperature.

Figure 4.1 shows the dependence of the conductivities of a-SiGe:H on the substrate temperature (190 – 350 °C) for undoped a-SiGe:H. The gas flow rate ratio of GeH₄/(GeH₄+SiH₄) was fixed at 0.09. It is seen that all of the dark-conductivity (σ_D), photo-conductivity (σ_{ph}) and the ratio of σ_{ph}/σ_D have large dependences on the substrate temperatures. The dark-conductivity increases as the substrate temperature increases, while the ratio of σ_{ph}/σ_D seems to have its maximum point (about 7×10^3 S/cm) at the substrate temperature of about 250 °C. The increase of the dark-conductivity was due to the decrease of the optical energy gap as shown in

figure 4.2. The decrease of the photo-conductivity at the substrate temperature above 300°C is due to the increase of the dangling bonds density [11].

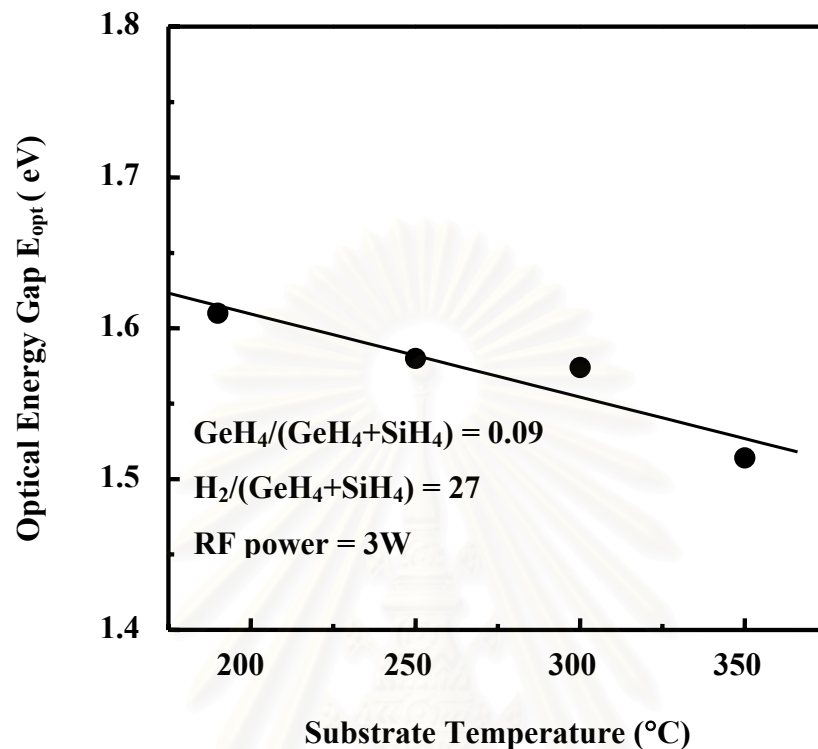


Figure 4.2 Dependence of the optical energy gap of undoped a-SiGe:H on the substrate temperature.

Figure 4.2 shows the dependence of the optical energy gap of undoped a-SiGe:H on the substrate temperature. The optical energy gap of a-SiGe:H decreases from about 1.60 eV to about 1.50 eV as the substrate temperature increases from 190 °C to 350 °C. The decrease of the optical energy gap with increasing the substrate temperature was due to the increase of the number of the localized states in the band-tail of a-SiGe:H.

4.3 Improvement of Photo-Conductivity of a-SiGe:H by Optimization of Gas Flow Rate Ratio of $H_2/(GeH_4+SiH_4)$

Another important preparation condition of hydrogenated amorphous silicon alloys in the plasma CVD method is the dilution of H_2 in the reaction gases. The electrical power applied through the RF electrodes is transferred to the gas phases and excites electrons for the decomposition of gases. The mean free-path and therefore the energy of free electrons in the gas depends on the pressure of the gas. From this point of view, in this work, a series of experiments has been done on the effect of the hydrogen gas dilution in the reaction gas on the photo-conductivity of undoped a-SiGe:H. In the experiments, the gas flow rate of H_2 was changed from 20 sccm to 250 sccm. The substrate temperature was fixed to the optimal 250°C as obtained from Figure 4.1. Table 4.2 summarizes the preparation conditions of undoped a-SiGe:H.

Table 4.2 Preparation conditions for undoped a-SiGe:H.

| | | |
|------------------------------------|--------|-------------------------------|
| RF power | 3 | watt (13.56 MHz) |
| Substrate temperature | 250 | °C |
| SiH ₄ gas flow rate | 50 | sccm (10% in H ₂) |
| GeH ₄ gas flow rate | 5 | sccm (10% in H ₂) |
| H ₂ gas flow rate | 20-250 | sccm |
| H ₂ gas flow rate ratio | y = | $H_2/(GeH_4+SiH_4)$ |

For simplicity, the H_2 gas flow rate ratio y is defined as $y = H_2/(GeH_4+SiH_4)$ as mentioned in Table 4.2.

Figure 4.3 shows the relationship between the conductivities of undoped a-SiGe:H and the H_2 gas flow rate ratio x. The substrate temperature in the Figure is fixed at 250 °C. For information, the total pressure of mixed gases in the reaction chamber is also shown on the upper horizontal axis.

It is found in the figure that the conductivities have large dependences on the H_2 gas flow rate ratio. One of the most important and interesting results obtained in the experiment is that the ratio of σ_{ph}/σ_D are as large as two to three orders of magnitude

in the whole range of the H₂ gas flow rate ratio. Another important and interesting result is that the H₂ gas flow rate ratio has an effect on the optical energy gap of the a-SiGe:H as shown in Figure 4.4.

Figure 4.4 shows the relationship between the optical energy gap (E_{opt}) of undoped a-SiGe:H and the H₂ flow rate ratio. Other preparation conditions including the substrate temperature = 250 °C, $\text{GeH}_4/(\text{GeH}_4+\text{SiH}_4) = 0.09$ have been fixed. It is interesting to point out that the optical energy gap of the undoped a-SiGe:H drastically decreases from about 1.6 eV to about 1.4 eV as the H₂ flow rate ratio increases from 12 to 54. By combining the results in Figures 4.3 and 4.4, we can obtain the relationship between the ratio of $\sigma_{\text{ph}}/\sigma_{\text{D}}$ and the optical energy gap of undoped a-SiGe:H as shown in Figure 4.5. In Figure 4.5, it is seen that the $\sigma_{\text{ph}}/\sigma_{\text{D}}$ slowly decreases from 10^4 and still keeping the value higher than 10^2 even though the optical energy of a-SiGe:H decreases from 1.6 eV to 1.4 eV.

If we combine the results in Figure 3.11 in chapter 3 with the results in this chapter, it is clearly seen that by optimizing the substrate temperature as well as the H₂ gas flow rate ratio, we can prepare undoped a-SiGe:H having high photo-conductivity and small optical energy gap.

Now we will discuss the reason why the optical energy gap of a-SiGe:H decreases when H₂ gas flow rate ratio increases. In the experiment, when the H₂ gas flow rate ratio increases, the total gas pressure in the reaction chamber also increases as indicated in Figure 4.3. (This is because fortunately the rotary pump in the CVD system has a small pumping speed.) It is generally known that if the pressure of gas in a glow discharge plasma system increases, the mean free path and the energy of free electrons in the plasma will decrease. Another important fact is that the energy necessary for the decomposition of GeH₄ is lower than that of SiH₄. Therefore, in the condition that the energy of free electrons is low, the efficiency of the decomposition of GeH₄ is higher than that of SiH₄. This means that in the higher gas pressure condition, GeH₄ gas is more easily decomposed than SiH₄ gas, and therefore, the Ge contents in a-SiGe:H are increased. Through these interpretations, it can be concluded that the optical energy gap of a-SiGe:H can be reduced by increasing the H₂ gas flow rate ratio. And the most important result that should be pointed out is that using the technique of dilution of H₂ gas in the reaction chamber, we can obtain a-SiGe:H with small optical energy gaps and high photo-conductivities.

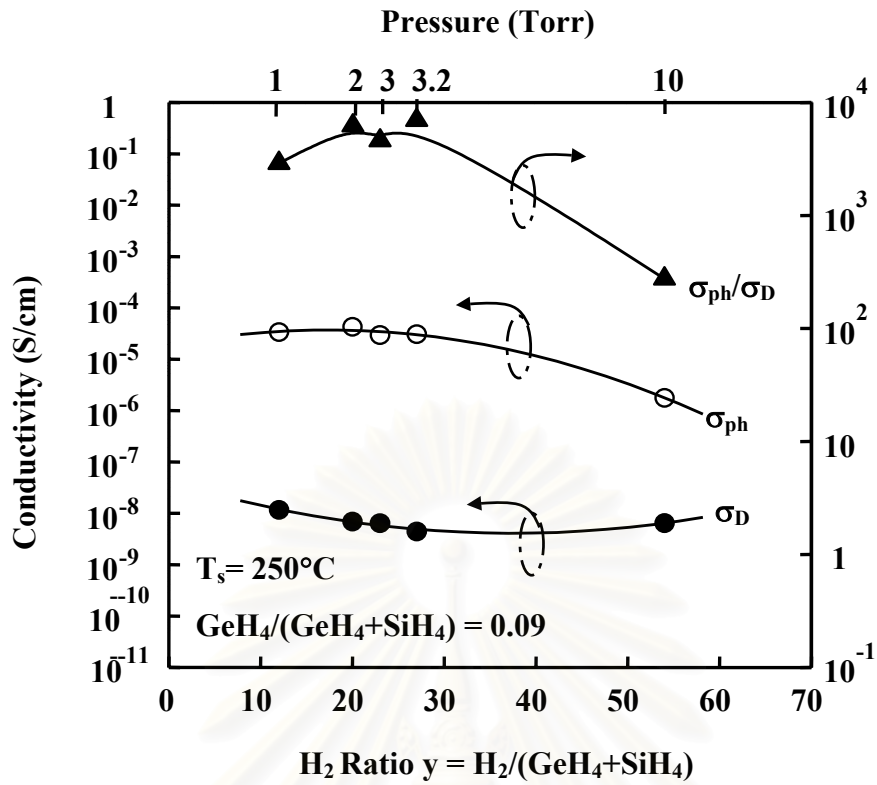


Figure 4.3 Relationship between conductivity and H₂ ratio of a-SiGe:H.

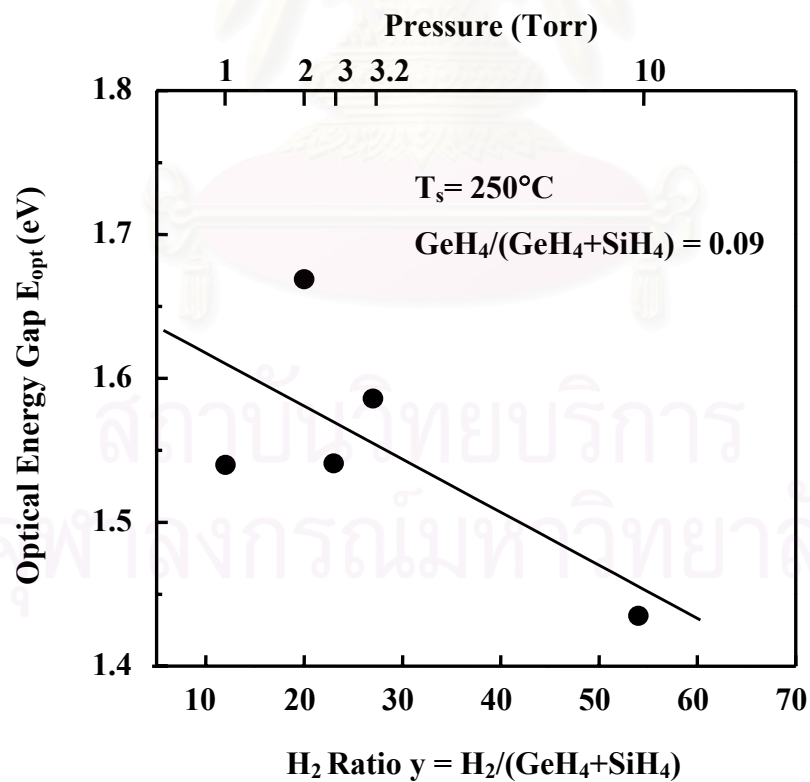


Figure 4.4 Dependence of the optical energy gap of undoped a-SiGe:H on H₂ gas flow rate ratio.

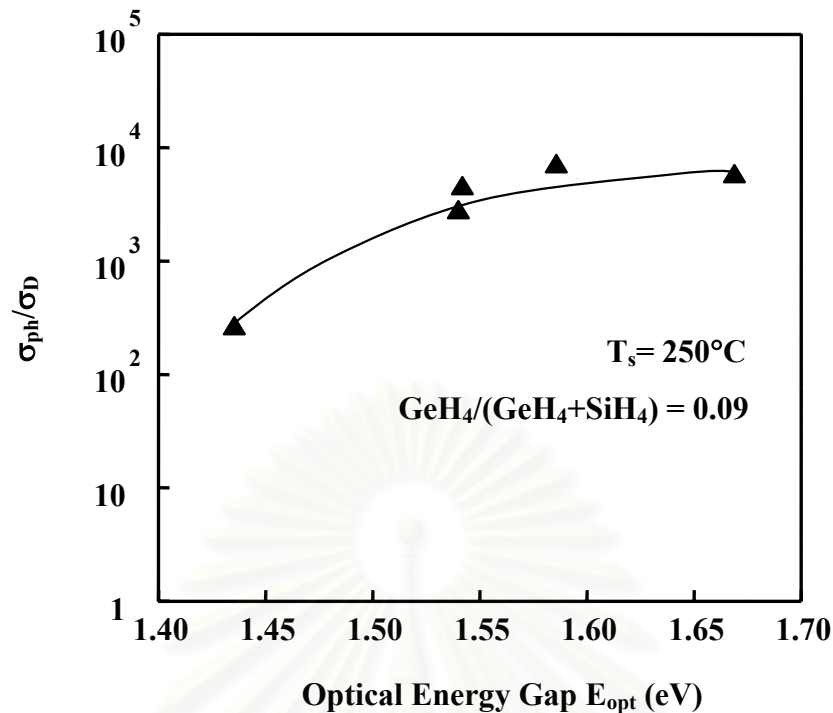


Figure 4.5 Relationship between the ratio of σ_{ph}/σ_D and the optical energy gap of undoped a-SiGe:H.

Summary

In this chapter, the improvement of the photo-conductivity (σ_{ph}/σ_D) of undoped a-SiGe:H has been successfully done by optimizing the substrate temperature and H_2 gas flow rate ratio. The interesting results obtained are as follows:

1. The optimal substrate temperature for the preparation of undoped a-SiGe:H having high photo-conductivity was about 250 °C.
2. The dark- and photo-conductivities of the a-SiGe:H prepared at 250 °C were 10^{-9} S/cm and 10^{-5} S/cm, respectively. These give the ratio of σ_{ph}/σ_D as high as 10^4 .
3. The optical energy gap of a-SiGe:H decreases from 1.63 eV to 1.50 as the substrate temperature increases from 190 °C to 350 °C.
4. The optimal H_2 gas flow rate ratio ($H_2/(GeH_4+SiH_4)$) for the preparation of a-SiGe:H having high photo-conductivity was about 20-30.

5. The ratio of σ_{ph}/σ_D as high as 10^4 was achieved with the H_2 gas flow rate ratio about 20-30.
6. It was found that the optical energy gap of a-SiGe:H can be reduced by adding H_2 gas in the reaction chamber.
7. A-SiGe:H having small optical energy gaps and high photo-conductivities can be obtained by mixing H_2 in the GeH_4+SiH_4 into the reaction chamber.
8. The a-SiGe:H prepared by the above technique has high quality enough to be used as an active intrinsic layer in the infrared-light thin film photodiode as will be described in chapter 5.



สถาบันวิทยบริการ
จุฬาลงกรณ์มหาวิทยาลัย

CHAPTER 5

Structure and Fabrication of Infrared-Light a-SiGe:H Thin Film Photodiode

5.1 Introduction

In chapter 4, it has been reported that a-SiGe:H having high photo-conductivities and small optical energy gaps could be successfully prepared by the conventional glow discharge plasma CVD. Some special techniques, e.g. optimization of the substrate temperature and mixing H₂ gas with high flow rate ratio have been adopted in the preparation of the a-SiGe:H. In this chapter, the application of the high quality a-SiGe:H as the photo-carrier generating i-layer in the p-i-n junction thin film photodiode is described. The fabrication of the a-SiGe:H photodiode and the results including the output characteristics are presented and discussed.

5.2 Structure of a-SiGe:H Thin Film Photodiode

The structure of the a-SiGe:H thin film photodiode fabricated in this work is glass/ITO/p-a-SiC:H/i-a-SiGe:H/n- μ c-SiC:H/Al as shown in Figure 5.1. The substrate was glass/ITO. The ITO stands for Indium Tin Oxide and acts as a transparent-conductive electrode. The basic structure of the photodiode is the p-i-n junctions of hydrogenated amorphous silicon based alloys. The p-type amorphous silicon carbide (p-a-SiC:H) has the optical energy gap of about 2.0 eV and acts as the wide gap window layer. The n-type microcrystalline silicon (n- μ c-Si:H) has the optical energy gap of about 1.8-1.9 eV. Aluminum (Al) is used as the back ohmic electrode. The thickness of each layer is shown Figure 5.1. The effective area of a photodiode is 0.033 cm².

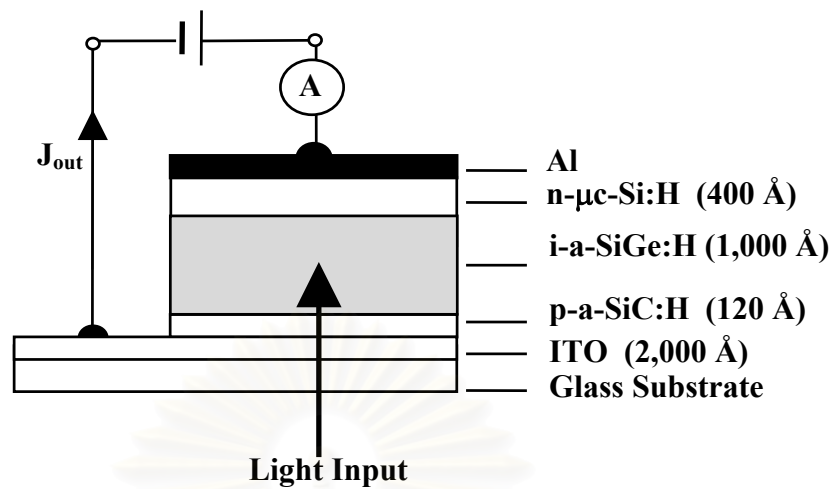


Figure 5.1 Basic structure of a-SiGe:H thin film photodiode.

Since the optical energy gap of the a-SiGe:H employed in the work is 1.4 –1.6 eV, the a-SiGe:H thin film photodiodes are sensitive to infrared light. Under a reverse bias condition and photons are incident on the device, electron-hole pairs are generated in the i-a-SiGe:H layer and electrons will be drifted by the electric field to the n-layer, while holes will be drifted to the p-layer. It will be described that the magnitude of the photo-current output depends on the reverse bias voltage, wavelength and intensity of the incident light.

5.3 Fabrication of a-SiGe:H Thin Film Photodiodes

The fabrication processes of a-SiGe:H thin film photodiodes are shown in Figure 5.2. The substrate size was 2 cm \times 2 cm. The deposition of p-a-SiC:H, i-a-SiGe:H and n- μ c-Si:H layers were done by the glow discharge plasma CVD method. Details of the glow discharge plasma CVD method have been described in chapter 2. Table 5.1 summarizes the preparation conditions of the p-i-n layers by the glow discharge plasma CVD method. The Al back electrode was deposited by the filament heat resistive evaporator. The shape of the Al electrode was a dot with the diameter of 2 mm. Figure 5.3 shows a picture of the a-SiGe:H photodiodes.

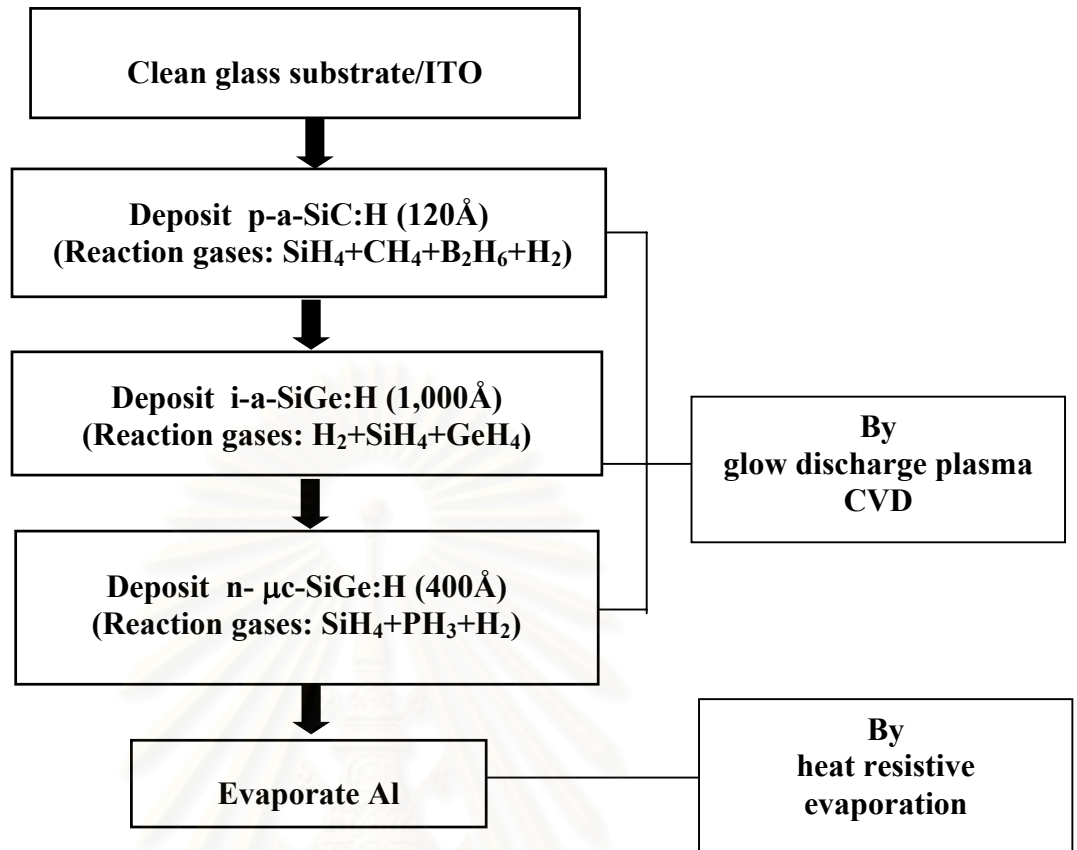


Figure 5.2 Fabrication process of a-SiGe:H thin film photodiode.

Table 5.1 Preparation conditions of p-i-n layers by the glow discharge plasma CVD method.

| Conditions | p-a-SiC:H Layer | i-a-SiGe:H Layer | n-μc-Si:H Layer |
|----------------------------|--|--|---|
| Substrate Temperature (°C) | 190 | 250 | 190 |
| RF Power (Watt) | 3 | 3 | 3 |
| Reaction Gases | SiH ₄ +CH ₄ +B ₂ H ₆ +H ₂ | H ₂ +SiH ₄ +GeH ₄ | SiH ₄ +PH ₃ +H ₂ |
| Optical Energy Gap (eV) | 2.0 | 1.4-1.6 | 1.8-1.9 |
| Thickness (Angstrom) | 120 | 1,000 | 400 |
| Dark-Conductivity (S/cm) | 10 ⁻⁷ | 10 ⁻⁹ | 1-10 |

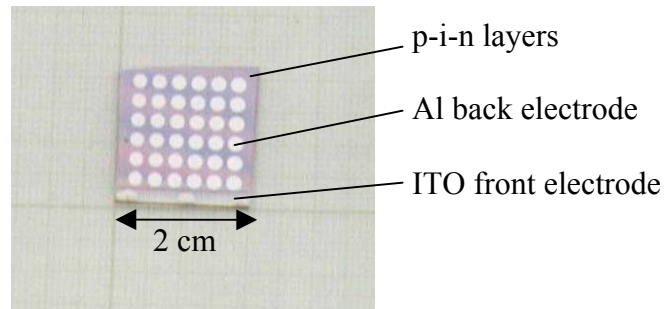


Figure 5.3 Picture of a-SiGe:H photodiodes.

The silver color dots are the Al back electrodes.

5.4 Basic Output Characteristics of a-SiGe:H Thin Film Photodiodes

Figure 5.4 shows examples of the I-V curves of two a-SiGe:H thin film photodiodes (TFPDs) having different optical energy gap a-SiGe:H layers (1.49 eV and 1.58 eV) in the dark and illuminated conditions. The light source of the illumination was the standard solar simulator (100 mW/cm², AM1).

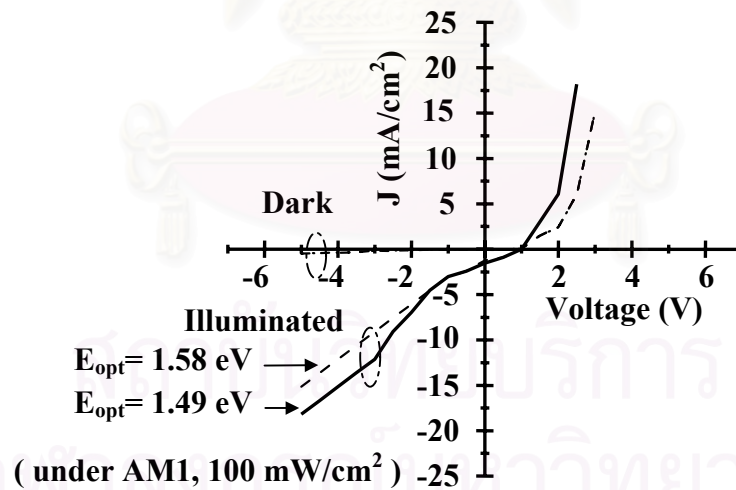


Figure 5.4 Examples of I-V curves of two a-SiGe:H thin film photodiodes having different optical energy gaps of a-SiGe:H. E_{opt} denotes the optical energy gap of a-SiGe:H i-layer.

In the figure, the dark currents of both devices at the reverse bias voltage of 5 V have been confirmed to be less than $10 \mu\text{A}/\text{cm}^2$. In the case of the photo-current, it is found that the photo-current outputs (in the 3rd quadrant) of the a-SiGe:H TFPDs strongly depend on the reverse bias voltages. For example, the photo-current outputs of the photodiodes at -2V are about 7-8 mA/cm^2 , and the photo-current outputs at -5 V are around 15 - 18 mA/cm^2 .

The strong dependences of the photo-current outputs on the reverse bias voltages of the a-SiGe:H thin film photodiode are due to the drift-type photovoltaic effect as similarly seen the case of a-Si:H thin film solar cell or a-Si:H thin film photodiode. This means that an external electric field has a strong influence on the collection efficiency of the photo-generated carriers. The effect is obviously observed in the case of a-SiGe:H thin film photodiode because of the small mobility and the small diffusion length of the photo-generated electrons and holes [15]. Figures 5.5 (a) – (c) show the schematic band diagrams of a-SiGe:H TFPD at the thermal equilibrium, weak reverse bias and strong reverse bias conditions.

In figure (b) , when a weak reverse bias is applied to the a-SiGe:H TFPD, most of the photo – generated carriers are trapped at the localized states, resulting in a small output signal. In figure (c), when a strong reverse bias is applied to the a-SiGe:H TFPD, a lot of the photo – generated carriers can flow to the output, resulting in a big output signal.

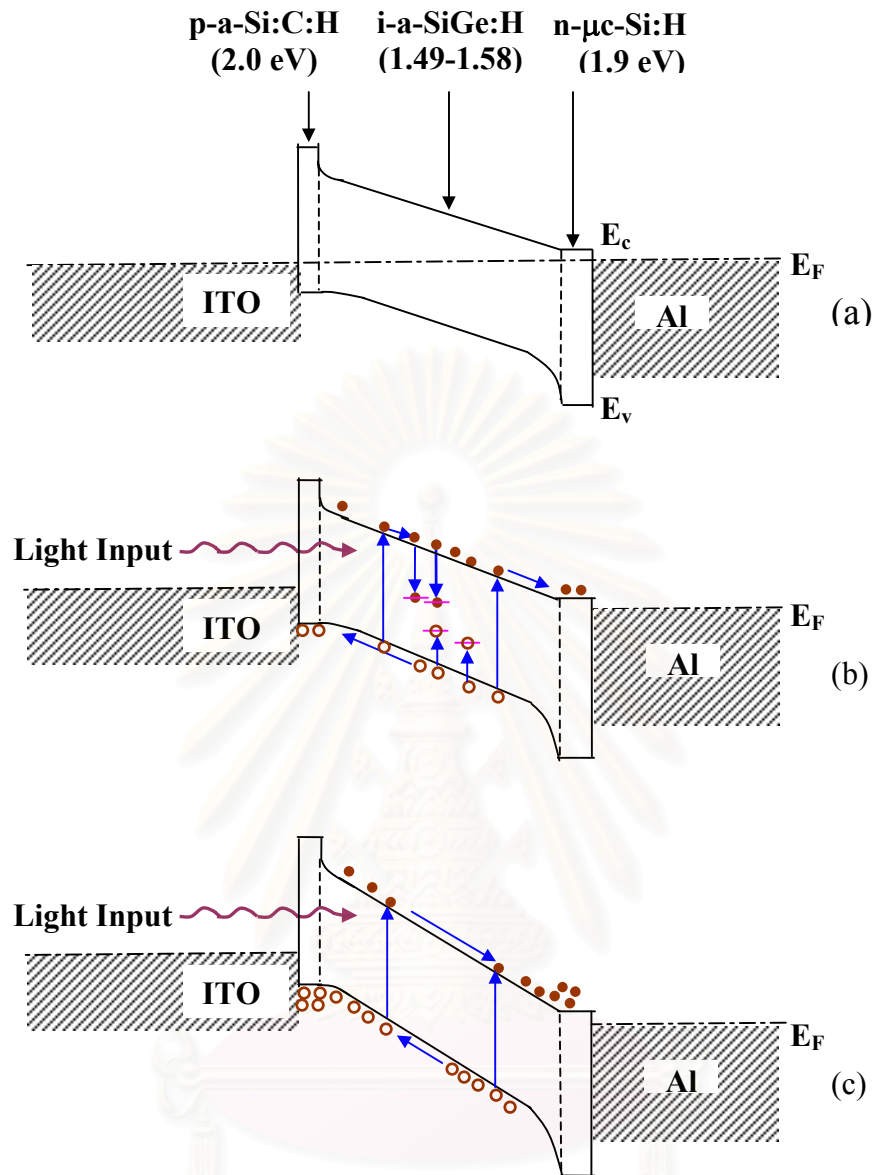


Figure 5.5 Schematic band diagrams of a-SiGe:H TFPD (a) thermal equilibrium (b) weak reverse bias and (c) strong reverse bias conditions.

Figure 5.6 shows the spectra of photo-current outputs of the two a-SiGe:H thin film photodiodes measured at room temperature. The optical energy gaps of the a-SiGe:H layers are 1.49 eV and 1.58 eV, respectively. The measurement used the lock-in amplifier technique. A 150 watt tungsten lamp was used as the light source. The peaks of the spectra in Figure 5.5 were normalized to become the same height. The spectrum response of a standard a-Si:H thin film photodiode in which the optical energy gap of i-layer is 1.89 eV is also shown for comparison.

As can be seen in Figure 5.6, the spectra of a-SiGe:H thin film photodiodes lie in the longer wavelength regions as compared with that of a-Si:H thin film photodiode. The a-SiGe:H thin film photodiodes have better responses to the infrared light in the wavelength of 700-900 nm than a-Si:H thin film photodiode.

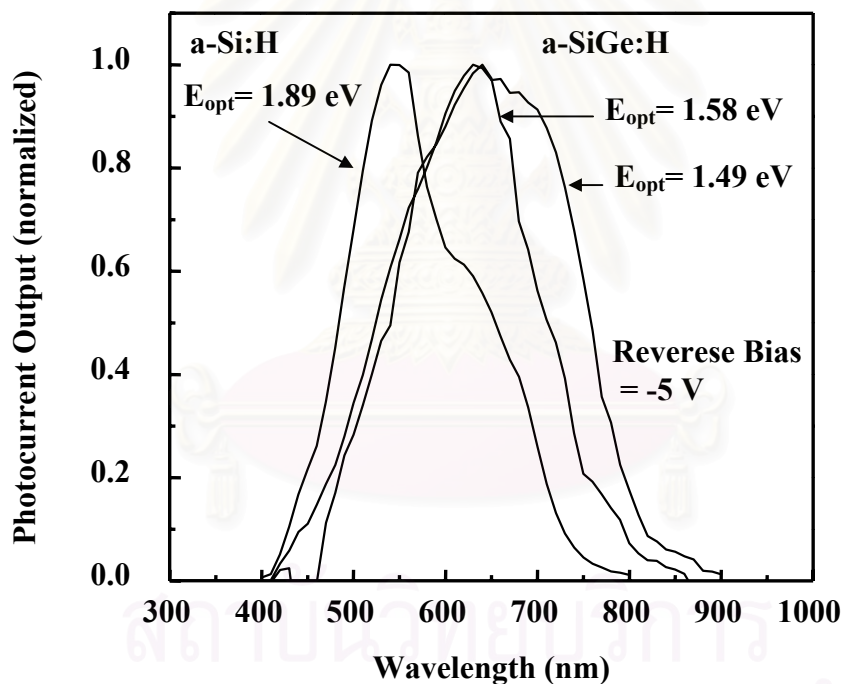


Figure 5.6 Spectrum responses of a-SiGe:H thin film photodiodes at room temperature. The spectrum of a-Si:H thin film photodiode is shown for comparison. E_{opt} denoted the optical energy gap of each photodiode.

Summary

The fabrications of infrared light a-SiGe:H thin film photodiodes have been described. The results are as follows:

1. The infrared light a-SiGe:H thin film photodiodes were successfully fabricated by the glow discharge plasma CVD method.
2. The photocurrent outputs of the a-SiGe:H thin film photodiodes having the optical energy gaps of a-SiGe:H about 1.49 – 1.58 eV have strong dependences on the reverse bias voltages. The photocurrent outputs are as high as 15 – 18 mA/cm² at the reverse bias of –5 V under the illumination of 100 mW/cm² (AM1 solar simulator). These values are comparable to that for the case of a conventional a-Si:H photodiode.
3. The a-SiGe:H thin film photodiodes have better responses to the infrared light with the wavelength of 700-900 nm as compared with that of a conventional a-Si:H thin film photodiode.
4. The a-SiGe:H thin film photodiodes are useful in the application of the light detecting devices in amorphous thin film photocouplers as will be described in chapter 6.

CHAPTER 6

Structures and Fabrications of Amorphous Thin Film Photocouplers Consisting of a-SiC:H Light Emitting Diode and a-SiGe:H Photodiode

6.1 Introduction

An amorphous photocoupler is a functional device, which transfers an electrical signal to an optical signal and also transfers the optical signal back to an electrical signal. The applications of the device are for example, interfaces for signal transmission, position and size detectors of moving objects, tape end detectors. It was reported that amorphous photocouplers consisting of a hydrogenated amorphous silicon carbide p-i-n thin film light emitting diode (a-SiC:H TFLED) and a hydrogenated amorphous silicon p-i-n thin film photodiode (a-Si:H TFPD) were fabricated [1]. So far the amorphous TFPD was made of a-Si:H, therefore it was mostly sensitive to the visible light. For this reason, the a-SiC:H TFLED must contain the i-a-SiC:H layer which had a large optical energy gap of more than 2.8 eV so that it could emit visible light (orange to white blue). However, the a-SiC:H TFLED which possesses such a large optical energy gap needs to be operated at a high voltage of 20-25 V.

A possible solution for decreasing the operating voltage of the TFLED is to reduce the optical energy gap of the i-a-SiC:H layer to about 2.2-2.5 eV. The i-a-SiC:H having an optical energy gap in this range emits the light from red to near infrared region. At the same time the optical energy gap of the intrinsic layer in the TFPD has to be decreased to about 1.5 eV which can be done by using hydrogenated amorphous silicon germanium (a-SiGe:H) material as the intrinsic layer in the TFPD.

In the previous chapters, the successes on the preparation of undoped a-SiGe:H having high photo-conductivity and the fabrication of a-SiGe:H TFPD by the glow discharge plasma CVD have been described.

In this chapter, a brief review on the usefulness of photocouplers will be described and followed by the presentations of the designs and fabrications of the amorphous photocouplers consisting of a-SiC:H thin film light emitting diodes and a-SiGe:H thin film photodiodes. The results will be shown that the amorphous photocouplers can be

operated in the infrared light regions and use lower voltages as compared with the visible amorphous photocouplers.

6.2 Usefulness of Photocouplers

A photocoupler is a functional optoelectronic device which consists of a light emitting device and light detecting device in a single sealed package to provide optical signal transmission. Electrical isolation is provided between input and output, and induction from external electro-magnetic field is eliminated between circuits of different impedance levels. As interface elements for signal transmission, photocouplers are widely used in office and factory automation equipment, as well as in all kinds of household appliances. Examples of the applications are interfaces between logic circuits, position & size detection of moving objects, tape end detection, I/O interfaces for computers, etc. [18]. Table 6.1 shows some examples of the applications of photocouplers. Figure 6.1 shows a picture of conventional crystalline photocouplers.

The conventional photocouplers have been made of crystalline semiconductors, such as GaAs, InP, Si, CdS, etc. so far. The disadvantages of these crystalline photocouplers are that they are made of expensive materials, small devices, hybrid devices, needs of different manufacturing technologies, such as Liquid Phase Epitaxy (LPE) for GaAs and Czochralski (CZ) for Si, etc.

Table 6.1 Examples of applications of photocouplers.

| |
|---|
| Interface between circuits with different voltages |
| Video signal transmission |
| High speed optical switch |
| Controlling speed of motor |
| Relay |
| Detection of telephone signal |
| Detection of rotation speed (video, laser disc, etc.) |
| Encoder |
| Detection of position in mouse |
| Measurement of size of materials |

| |
|------------------------------|
| Optical communication system |
| Counting number of materials |
| Electrography copy machine |

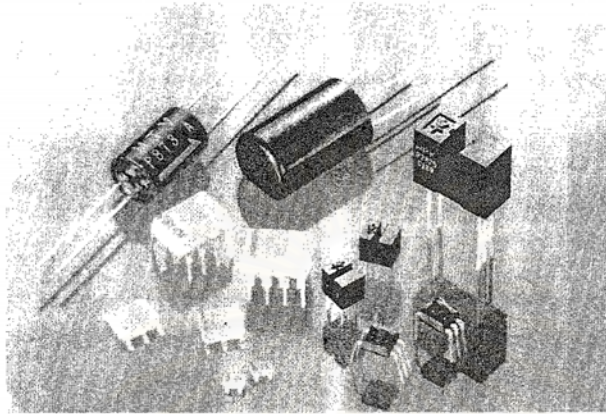


Figure 6.1 Picture of conventional crystalline photocouplers.

6.3 Structures of Conventional Amorphous Thin Film Photocouplers

The amorphous photocouplers consisting of a hydrogenated amorphous silicon carbide p-i-n thin film light emitting diode (a-SiC:H TFLED) and a hydrogenated amorphous silicon p-i-n thin film photodiode (a-Si:H TFPD) have been firstly reported by D. Kruangam et al [1, 16]. Figure 6.2 shows some examples of the structures of a-SiC:H/a-Si:H photocouplers. Figure 6.3 shows examples of the packages of amorphous photocouplers, and Figure 6.4 shows the pictures of the amorphous photocouplers fabricated in the previous works [18].

สถาบันวิทยบริการ
จุฬาลงกรณ์มหาวิทยาลัย

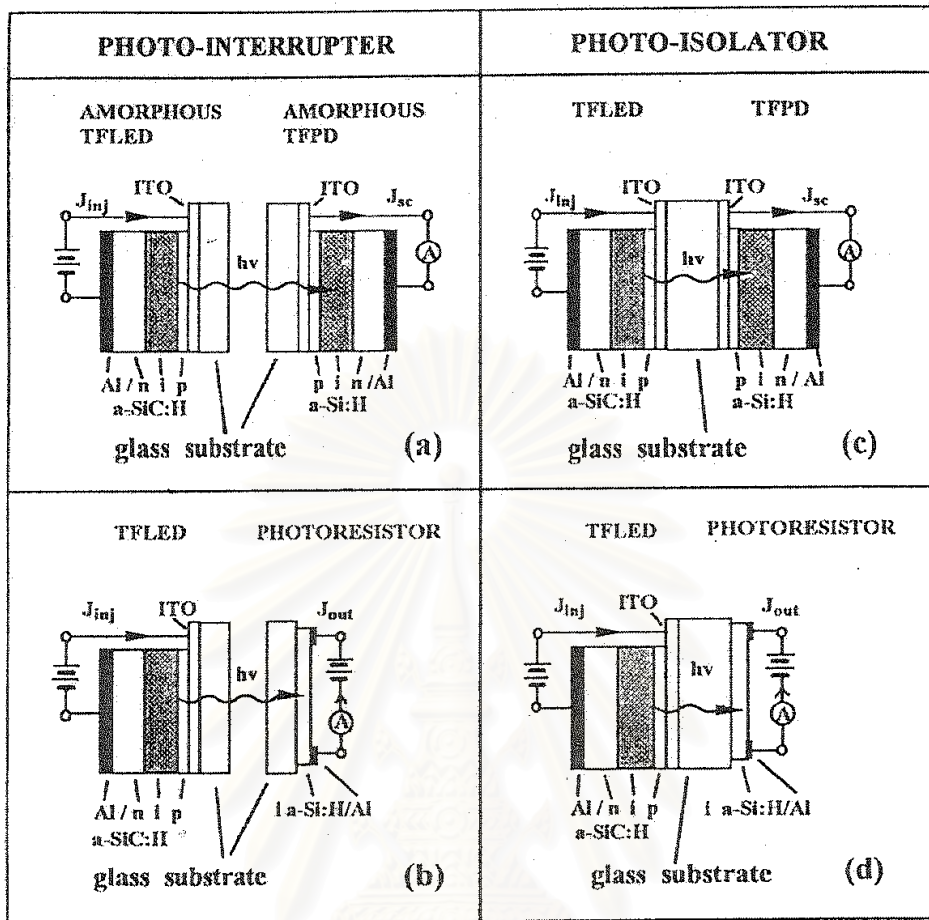


Figure 6.2 Structures of a-SiC:H/a-Si:H photocouplers.

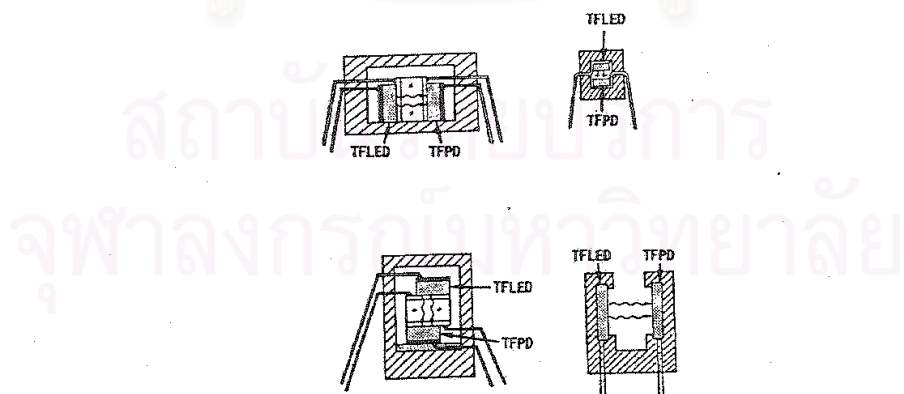


Figure 6.3 Examples of packages of amorphous photocouplers.

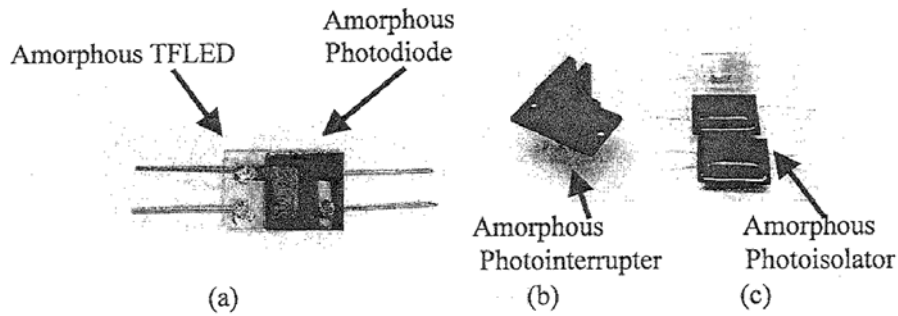


Figure 6.4 Pictures of a-SiC:H/a-Si:H photocouplers [18].

6.4 Development of a-SiC:H/a-SiGe:H Photocouplers

So far the amorphous thin film photodiode (TFPD) has been made of a-Si:H. Therefore, it is mostly sensitive to the visible light. For this reason, the a-SiC:H thin film light emitting diode (TFLED) had to contain the i-a-SiC:H layer which had a large optical energy gap of more than 2.8 eV so that it could emit visible light (orange to white blue color). The a-SiC:H TFLED which possesses such a large optical energy gap needs the operating voltage as high as 20-25 V resulting in short operating life time.

A solution for decreasing the operating voltage and also improving the lifetime of the TFLED is to reduce the optical energy gap of the i-a-SiC:H layer to about 2.2 – 2.5 eV. The i-a-SiC:H having the optical energy gap in this range emits red - near infrared light. And at the same time the optical energy gap of the intrinsic layer in the TFPD has to be decreased to about 1.4 –1.6 eV, and this can be done by using hydrogenated amorphous silicon germanium (a-SiGe:H) material as the intrinsic layer in the TFPD.

In this work, two types of a-SiC:H/a-SiGe:H photocouplers were designed and fabricated. Figures 6.5 (a) and (b) show the structures of the photocouplers.

- The photocoupler type (a) consists of an a-SiC:H p-i-n junction TFLED and an a-SiGe:H p-i-n junction thin film photodiode (TFPD). The TFPD is operated under a reverse bias voltage. The advantage of type (a) is the fast response time as compared with type (b). But the magnitude of the output signal of the TFPD is low due to the low quantum efficiency of the TFPD.
- The photocoupler type (b) consists of an a-SiC:H p-i-n junction TFLED and an a-SiGe:H photoresistor. The photoresistor needs ohmic contacts and the operation voltage can be changed in a wide range so that the quantum efficiency is higher than that of type (a). But the disadvantage of type (b) is a slow response time as compared with type (a).

In the sections 6.4.1 and 6.4.2, the fabrications of a-SiC:H TFLEDs and a-SiGe:H TFPD, respectively, will be presented.



สถาบันวิทยบริการ
จุฬาลงกรณ์มหาวิทยาลัย

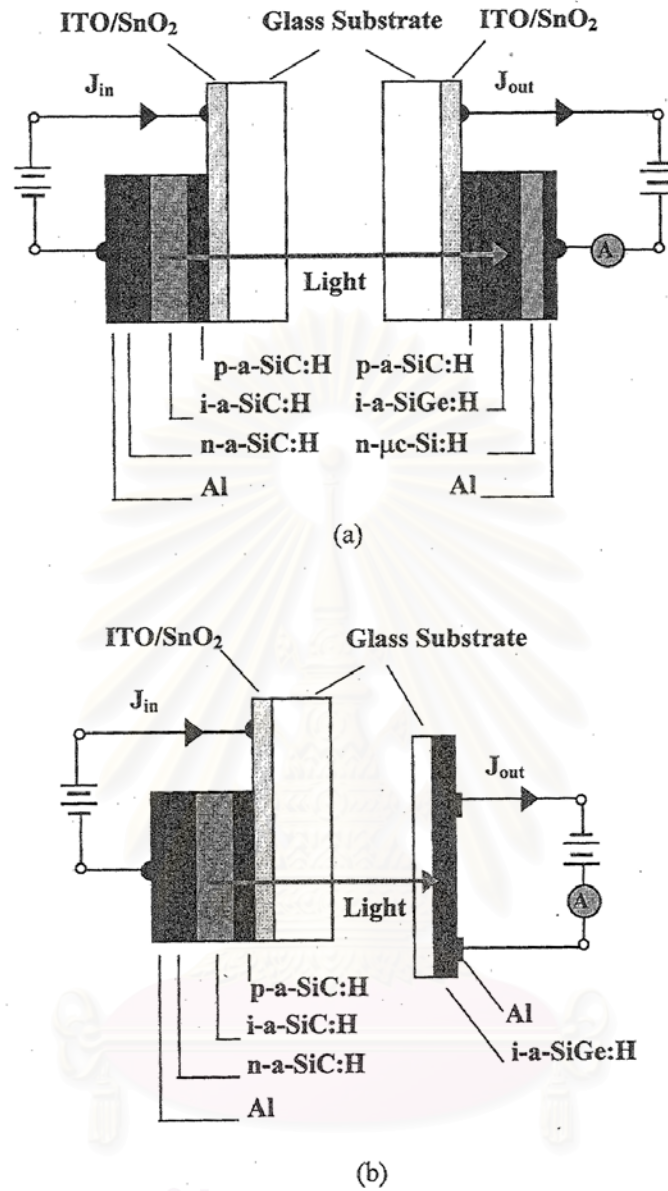


Figure 6.5 Structures of amorphous photocouplers having an a-SiC:H TFLED as a red color-near infrared light emitting device. Type (a) uses a-SiGe:H thin film photodiode as a light detector. Type (b) uses a-SiGe:H photoresistor as a light detector.

6.4.1 Fabrication of a-SiC:H Thin Film Light Emitting Diodes

The amorphous photocouplers developed in the work use the a-SiC:H TFLEDs as light emitting devices. The structure of the a-SiC:H TFLED is the p-i-n junctions of a-SiC:H as shown in Figure 6.6. The substrate is glass/ITO/SnO₂. The back electrode is Al. The a-SiC:H p-i-n layers were prepared by the glow discharge plasma CVD method with the conditions shown in Table 6.2. The substrate temperature was 190°C and the RF power density was 12 mW/cm².

Table 6.2 Fabrication conditions of a-SiC:H p-i-n junction thin film LEDs (TFLEDs) by the glow discharge plasma CVD.

| | |
|-----------------------|---|
| Substrate temperature | 190 °C |
| RF power density | 12 mW/cm ² |
| p-a-SiC:H layer | Gases CH ₄ +SiH ₄ +B ₂ H ₆ +H ₂ Optical energy gap = 2.0 eV Thickness = 120 angstrom |
| i-a-SiC:H layer | Gases C ₂ H ₄ +SiH ₄ +H ₂ Optical energy gap = 2.36 eV Thickness = 500 angstrom |
| n-a-SiC:H layer | Gases CH ₄ +SiH ₄ +PH ₃ +H ₂ Optical energy gap = 2.0 eV Thickness = 500 angstrom |

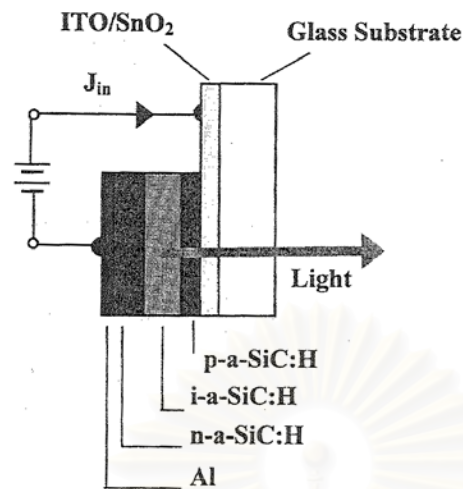


Figure 6.6 Structure of amorphous silicon carbide (a-SiC:H) thin film light emitting diode.

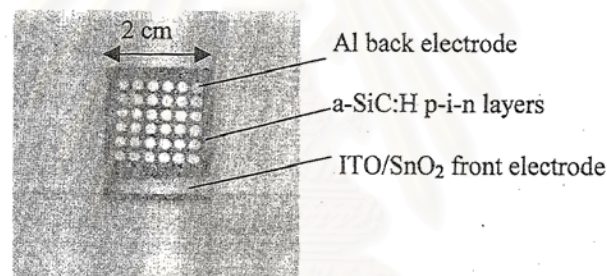


Figure 6.7 Picture of the a-SiC:H thin film light emitting diodes fabricated on a glass substrate. The white color dots are the back Al electrodes. The transparent area is the front ITO/SnO₂ electrode.

Figure 6.8 shows the $I(V)$ curves of a-SiC:H TFLEDs having different optical energy gaps of the i-layers. The E_{opt} denotes the optical energy gap of the i-layer. It is interesting to point out that the threshold voltages of the TFLEDs decrease as the optical energy gaps decrease. For example, the threshold voltage of the 2.36 eV TFLED is about 7 V.

The decrease of the threshold voltage with the decrease of the optical energy gap of the i-a-SiC:H layer can be explained as follows. It has been studied and reported in details [17] that the carrier injection mechanism in the a-SiC:H TFLED is based upon

the tunneling of electrons and holes through the notch barriers at the i/n and p/i interfaces, respectively because the optical energy gap of the i-layer is wider than those of the p- and n-layers. If the optical energy gap of the i-layer decreases, the tunneling efficiency of the carriers will increase, and therefore, the voltage necessary for the tunneling is reduced.

The results in Figure 6.8 suggest that the forward bias voltage for the operation of the TFLED can be reduced by decreasing the optical energy gap of the luminescent i-layer. Once when the forward bias voltage is reduced, the operation lifetime of the TFLED should be extended.

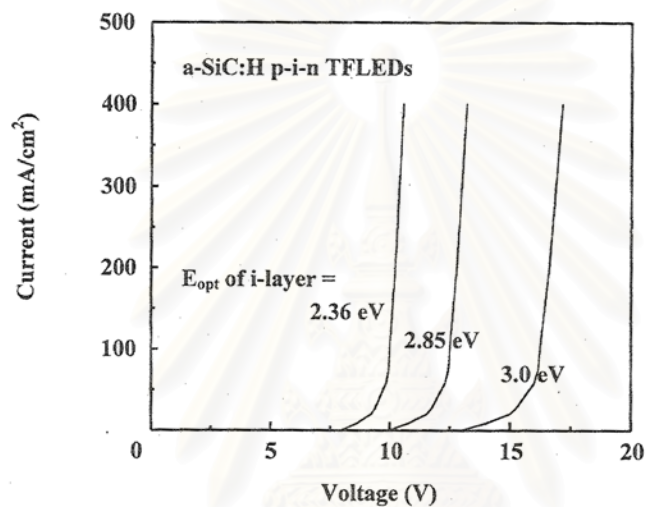


Figure 6.8 I(V) curves of a-SiC:H TFLEDs having different optical energy gaps of the i-layers.

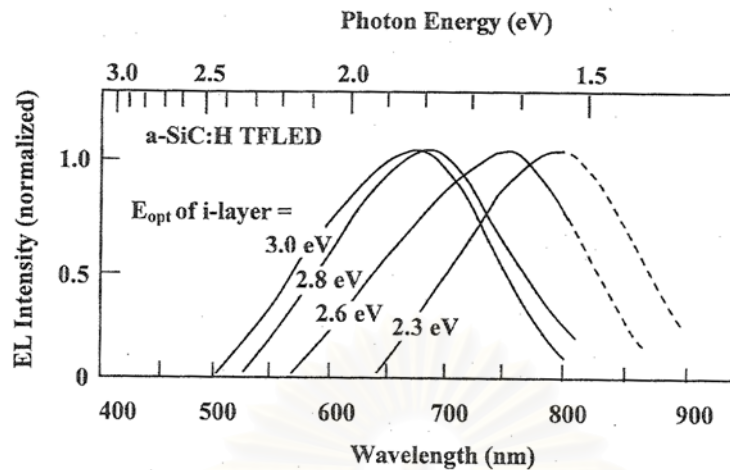


Figure 6.9 Room temperature electroluminescent spectra of a-SiC:H TFLEDs.

The parameter is the optical energy gap of the i-layer. Dash lines denote the extrapolation due to the limitation of the sensitivity of the measurement system.

Figure 6.9 shows the room temperature electroluminescent spectra of a-SiC:H TFLEDs. The parameter is the optical energy gap of the i-layer (2.36, 2.8, 3.0 eV). The spectra of these samples have large full width at half maximum (FWHM) about 0.4 – 0.5 eV. The peak positions of all samples have the photon energies below the optical energy gaps, because the radiative recombinations of electrons and holes occur at the deep localized states in the energy gaps.

It has been reported [18] that the a-SiC:H TFLEDs have the cut-off frequency around 500 kHz. The definition of the cut-off frequency is the frequency at which the intensity of light is 70% of the value at low frequency. The result implies that the a-SiC:H TFLEDs can respond fast enough to the pulse current input with the frequency up to around 500 kHz.

6.4.2 Fabrication of a-SiGe:H Thin Film Photodiodes

The details of the fabrication of a-SiGe:H films, a-SiGe:H thin film photodiodes as well as the results have been described in details in chapters 2-5. In this section, brief description on the fabrication of the a-SiGe:H thin film photodiode for the purpose of the application as a light detector in the photocoupler will be given.

Undoped a-SiGe:H films were prepared by the glow discharge plasma CVD system from the GeH₄, SiH₄ and H₂ gas mixture. The typical preparation conditions of a-SiGe:H are summarized in Table 6.3. The thicknesses of the p-i-n layers in the thin film photodiode (TFPD) are 120 Å, 1,000 Å and 400 Å, respectively. Glass/ITO (1,800 Å)/SnO₂ (200 Å) sheets were used as the substrates.

In the case of the a-SiGe:H photoresistors, the thickness of the a-SiGe:H is about 7,550 Å. Co-planar Al electrodes were deposited on the a-SiGe:H with the 1 mm distance and 1.7 mm length.

Table 6.3 Preparation conditions of undoped a-SiGe:H films.

| | |
|-----------------------|--|
| Substrate temperature | 250 °C |
| Pressure | 1-3 torr |
| Back ground pressure | 0.01 torr |
| RF power density | 12 mW/cm ² |
| Gases | GeH ₄ + SiH ₄ + H ₂ |

6.5 Basic Characteristics of a-SiC:H/a-SiGe:H Thin Film Photocouplers

Figure 6.10 shows the relationship between the photocurrent output of the a-SiGe:H TFPD and the injection current density of the a-SiC:H TFLED for the amorphous photocoupler type (a) in Figure 6.5. The optical energy gap of the i-a-SiC:H layer in the TFLED is 2.36 eV and the emitting spectrum covers red color to near infrared regions. The photocurrent output of the TFPD linearly increases from $0.2 \mu\text{A}/\text{cm}^2$ to $1 \mu\text{A}/\text{cm}^2$ as the injection current density of the TFLED increases from $180 \text{ mA}/\text{cm}^2$ to $500 \text{ mA}/\text{cm}^2$. Therefore, the current transfer ratio (defined as J_{out} of TFPD divided by J_{inj} of TFLED) of the amorphous photocoupler is estimated to be about $10^{-4} \%$.

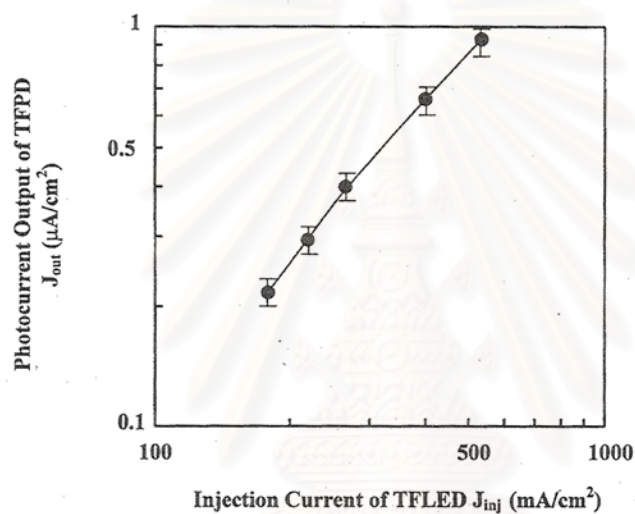


Figure 6.10 Relationship between the photocurrent output of the a-SiGe:H TFPD and the injection current density of a-SiC:H TFLED constructed in the amorphous photocoupler type (a). The distance between the TFLED and the TFPD is 4 mm. The area of both device is 0.017 cm^2 . The line is drawn as a guide for the eyes.

สถาบันวิทยบริการ
จุฬาลงกรณ์มหาวิทยาลัย

Figure 6.11 shows the relationship between the photocurrent output and the applied voltage of the a-SiGe:H photoresistor ($E_{opt} = 1.49$ eV) used in the amorphous photocoupler type (b) in Figure 6.5. The parameter in the Figure is the injection current density of the a-SiC:H TFLED. The distance between the TFLED and the photoresistor is 2 mm. It is found that the photocurrent output of the a-SiGe:H photoresistor has a strong and linear dependence on the applied voltage of the photoresistor. It is interesting to point out that one feature of the photoresistor is that the gain of the output (defined as the ratio of photocurrent to dark current) can be enlarged by increasing the voltage applied to the photoresistor.

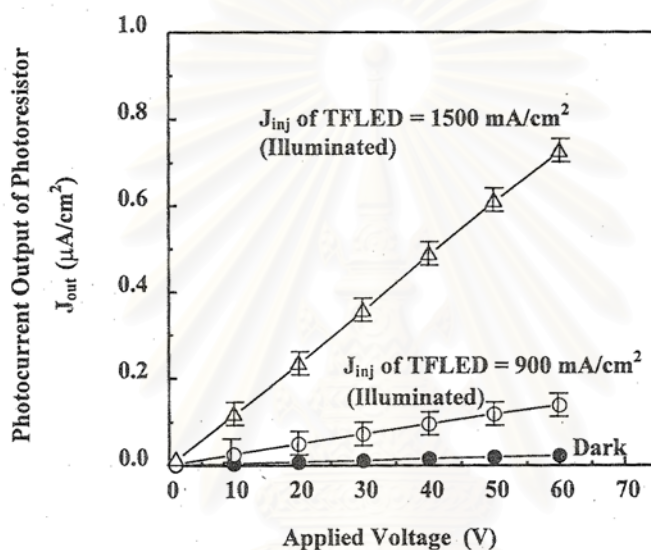


Figure 6.11 Relationship between the photocurrent output and applied voltage of a-SiGe:H photoresistor which is illuminated by the light from a-SiC:H TFLED. The distance between the photoresistor and the TFLED is 2 mm. The parameter is the injection current density of the a-SiC:H TFLED. The lines are drawn as guides for the eyes.

Although the brightness of the a-SiC:H TFLED is still as low as $0.1 - 1$ cd/m² which is too low for any application as a display, it is shown in the work that the a-SiC:H TFLED can be applied as a light source of a photocoupler. As seen in chapter 5 and as will be described in chapter 7, even though the a-SiGe:H TFPDs have very poor

photovoltaic characteristics, the TFPDs can give high photocurrent output density when they are operated with reverse bias conditions.

In the previous works [18], the optical energy gap of the i-a-SiC:H layer in the p-i-n junction TFLED was as large as 3.0 eV, which caused the operating lifetime of the TFLED was as short as several minutes. On the other hand, since the optical energy gap of the i-a-SiC:H layer of the TFLED in the work has been reduced to be only 2.36 eV, the operating lifetime of the TFLED and therefore of the amorphous photocoupler has been largely improved to be several hours and days.

Summary

New types of amorphous photocouplers consisting of a-SiC:H thin film light emitting diodes, a-SiGe:H thin film photodiodes and a-SiGe:H photoresistors have been developed. The results can be summarized as follows:

- 1) New types of amorphous photocouplers consisting of a-SiC:H thin film light emitting diodes, a-SiGe:H thin film photodiodes and a-SiGe:H photoresistors had been developed.
- 2) The operating voltage of the a-SiC:H TFLEDs was decreased by using a-SiC:H with the small optical energy gap of 2.36 eV.
- 3) The lifetime of the a-SiC:H TFLEDs has been improved by using small optical energy gap a-SiC:H.
- 4) These two types of photocouplers operates in the infrared light range since the a-SiGe:H TFPD and a-SiGe:H photoresistor had the spectral responses in 700-900 nm.
- 5) The current transfer ratio (defined as J_{out} of TFPD divided by J_{inj} of TFLED) of the amorphous photocoupler using a TFPD was estimated to be about 10^{-4} %.
- 6) High H_2 gas flow ratio and high substrate temperature at 250 °C were the key technologies to achieve a-SiGe:H with excellent photoconductivity.
- 7) It is expected the a-SiGe:H thin film photodiodes and the amorphous photocouplers proposed in the work will be useful in various optoelectronic applications.

- 8) In the next chapter, a-SiGe:H thin film will be applied as the active layer in the amorphous thin film solar cell. Some results of the preliminary experiments including the output characteristics will be presented and discussed.



สถาบันวิทยบริการ
จุฬาลงกรณ์มหาวิทยาลัย

Chapter 7

Conclusions

A series of experiments on the study of the basic properties of a-SiGe:H thin films has been done. The a-SiGe:H was applied as an intrinsic active layer in infrared light amorphous thin film photodiode. The a-SiGe:H thin film photodiode was employed as the light detecting device in the amorphous photocoupler. The conclusions of the work are as follows.

1. A-SiGe:H thin films were successfully fabricated by the glow discharge plasma CVD method using SiH₄, GeH₄ as the reactive gases and H₂ as the diluent.
2. According to the results of the infrared absorption spectra, it is found that there are several atomic bonding in a-SiGe:H, e.g., Si-H_x, Ge-H_y, Si-Ge, etc. The increase of Ge contents can be achieved by increasing the gas flow rate ratio of GeH₄/(GeH₄+SiH₄).
3. The optical energy gap of a-SiGe:H decreases from about 1.8 eV to 1.1 eV as the ratio of $x = \text{GeH}_4/(\text{GeH}_4+\text{SiH}_4)$ increase from 0.09 to 0.83. These results show that the optical energy gaps of a-SiGe:H can be widely changed by adjusting the ratio of x.
4. The results of the measurement of ESR show that the dangling bond density in a-SiGe:H increases as the gas flow rate ratio $x = \text{GeH}_4/(\text{GeH}_4+\text{SiH}_4)$ increases (also as the Ge contents increase). Therefore, the photo-conductivity of a-SiGe:H decreases as the optical energy gap decreases.
5. The dark-conductivity of undoped a-SiGe:H increases from 10⁻¹⁰ to 10⁻⁴ S/cm as the gas flow rate ratio $x = \text{GeH}_4/(\text{GeH}_4+\text{SiH}_4)$ increases from 0.09 to 0.83. The increase of the dark-conductivity with Ge contents, is due to the decrease of the optical energy gap of a-SiGe:H and the shift of Fermi level towards the conduction band.
6. The ratio of photo-conductivity to dark-conductivity ($\sigma_{\text{ph}}/\sigma_{\text{D}}$) is in the order of 10³ only when the ratio of $\text{GeH}_4/(\text{GeH}_4+\text{SiH}_4)$ is as small as 0.09. The ratio of $\sigma_{\text{ph}}/\sigma_{\text{D}}$ drastically decreases to less than 10 when the ratio of $\text{GeH}_4/(\text{GeH}_4+\text{SiH}_4)$ is greater than about 0.5. The large decrease of the $\sigma_{\text{ph}}/\sigma_{\text{D}}$ with increasing

$\text{GeH}_4/(\text{GeH}_4+\text{SiH}_4)$ is considered to be due to the large increase of the dangling bond density in a-SiGe:H.

7. The improvement of photo-conductivity of a-SiGe:H was done by the optimization of substrate temperature. The optimal substrate temperature for high photo-conductivity a-SiGe:H was about 250 °C. The dark- and photo-conductivities of the a-SiGe:H prepared at 250 °C were 10^{-9} S/cm and 10^{-5} S/cm, respectively. These give the ratio of $\sigma_{\text{ph}}/\sigma_{\text{D}}$ as high as 10^4 .
8. The optical energy gap of a-SiGe:H decreases from 1.63 eV to 1.50 eV as the substrate temperature increases from 190 °C to 350 °C.
9. A-SiGe:H having small optical energy gaps and high photo-conductivities can be obtained by mixing H_2 in the reaction gases; $\text{GeH}_4+\text{SiH}_4$. The optimal H_2 gas flow rate ratio ($\text{H}_2/(\text{GeH}_4+\text{SiH}_4)$) was found to be about 20-30.
10. The infrared light a-SiGe:H thin film photodiodes were successfully fabricated by the glow discharge plasma CVD method.
11. It has been found that the photo-current outputs of the a-SiGe:H thin film photodiodes have strong dependence on the reverse bias voltages. The photo-current outputs are as high as 18 mA/cm² at the reverse bias of -5 V under the illumination of 100 mA/cm² (AM1 solar simulator). The a-SiGe:H thin film photodiodes have better responses to the infrared light with the wavelength of 700-900 nm as compared with a conventional a-Si:H thin film photodiode.
12. New types of amorphous photocouplers consisting of a-SiC:H thin film light emitting diodes, a-SiGe:H thin film photodiodes and a-SiGe:H photoresistors have been developed. The photocouplers operates in the infrared light range since the a-SiGe:H photodiode and photoresistor have the high spectral responses in the range of 700-900 nm.
13. The current transfer ratio (defined as J_{out} of TFPD divided by J_{inj} of TFLED) of the amorphous photocoupler was estimated to be about 10^{-4} %.
14. It is expected the a-SiGe:H thin film photodiodes and the amorphous photocouplers developed in the work are useful in various optoelectronic applications.

REFERENCES

- [1] Kruangam, D., Boonkosum, W., Ratwises, B., Panyakeow, S., and Delong, B. Visible-Light Amorphous Silicon Alloys Thin Film Light Emitting Diodes and its Applications to Optoelectronic Functional Devices. Proceedings of Eighth International School on Condensed Matter Physics (ISCMP), -Electronic, Optoelectronic and Magnetic Thin Films, Bulgaria, (1994): 87.
- [2] Petr, S., Pavel, S., Marie, T., and Pere, C. The Hydrogen Effusion Structural Changes and Defects in Hydrogenated Amorphous SiGe Films : Dependence Upon the Microstructure. J. Non Cryst. Solids, 227-230 (1998) 437-441.
- [3] Masaki, S., Akira, T., Masao, I., Hisao, H., and Makoto, T. Effects of Very High Hydrogen Dilution at Low Temperature on Hydrogenated Amorphous Silicon Germanium. J. Non Cryst. Solids, 227-230 (1998) 442-446.
- [4] Panlinginis, K.C., Cohen, J.D., Yang, J.C., and Guha, S. Defect Bands in a-Si-Ge:H Alloys with Low Ge Content. J. Non Cryst. Solids, 266-269 (2000): 665-669.
- [5] Wickboldt, P., Pang, D., Paul, W., Chen, J.H., Zhong, F., Cohen, J.D., Chen, Y., and Willianson, D.L. Improved a-Si_{1-x}Ge_x:H of large x Deposited by PECVD. J. Non Cryst. Solids, 198-200 (1996) 567-571.
- [6] Ganguly, G., and Matsuda, A. Role of Hydrogen Dilution in Improvement of a-SiGe:H Alloys. J. Non Cryst. Solids, 198-200 (1996) 559-562.
- [7] Yukimoto, Y. Hydrogenated a-SiGe Alloy and Its Optoelectronic Properties. Japanese Annual Review on Electronics and Computer Technologies (JARECT), Vol.6, Amorphous Semiconductor Technologies & Devices (1983), Y.Hamkawa (ed.): 136-147.
- [8] Street, R.A., and Knight, J.C. Luminescent in Plasma-Deposited Si-O Alloys, Phil. Mag. B42 (1980): 5551.
- [9] Carious, R., Fischer, R., Holzenkampfer, E., and Stuke, J. Photoluminescence in the Amorphous System SiO_x. J. Appl. Phys. 52 (1981): 4241.

- [10] Taylor, P.C. Information on Gap States in a-Si:H from ESR and LESR. Properties of Amorphous Silicon and Its Alloys, Tim Searle (ed.), EMIS Datareview Series, The Institution of Electrical Engineers, (UK) (1995): 139-142.
- [11] Werner, L., and Simon T. Hydrogenated Amorphous Silicon Alloy Deposition Processes. Marcel Dekker, Inc. (New York) (1993): 27-44.
- [12] Finger, F. and Beryer, W. Growth of a-SiGe:H Alloys by PECVD – Gas Source Condition in the Plasma and at the Interface. Properties of Amorphous Silicon and Its Alloys, Tim Searle (ed.), EMIS Datareview Series, The Institution of Electrical Engineers, (UK) (1995): 20-29.
- [13] Donald L. Smith. Thin-film Deposition, Principles & Practice. International edition. McGraw-Hill, Inc.(1995): 200-202.
- [14] Werner L., and Simon T. Hydrogenated Amorphous Silicon Alloy Deposition Processes. Marcel Dekker Inc., (New York) (1993): 45-56.
- [15] Adriaenssens, G.J. Mobilities in a-Si:H and Its Alloys,. Properties of Amorphous Silocon and Its Alloys. Tim Searle (ed.), EMIS Datareview Series, The Institution of Electrical Engineers, (UK) (1995): 199-208.
- [16] Boonkosum, W., Kruangam, D., Panyakeow, P., and DeLong, B. Novel Amorphous Photocoupler Consisting of a-SiC:H Thin Film LED and a-Si:H Thin Film Photodiode. 1994 Spring Meeting, Materials Research Society Symposium A. San Francisco, U.S.A. (1994).
- [17] Kruangam, D. Amorphous and Microcrystalline Silicon-Carbide Alloy Light Emitting Diodes, in J. Kanicky (ed.) Amorphous and Microcrystalline Semiconductor Devices: Optoelectronic Devices. Artech House, (Boston, London) (1991): 165-240.
- [18] Boonkosum, W. Visible- Light Amorphous Silicon Alloy Thin Film Light emitting Diodes and Their Applications in Optoelectronics. Doctoral dissertation, Department of Electrical Engineering, Chulalongkorn University, Thailand, 1996.

- [18] Boonkosum, W. Visible- Light Amorphous Silicon Alloy Thin Film Light Emitting Diodes and Their Applications in Optoelectronics. Doctoral dissertation, Department of Electrical Engineering, Chulalongkorn University, Thailand, 1996.
- [19] Carlson, D.E., and Wronski, C.R., Amorphous Silicon Solar Cell. Appl. Phys. Lett. Vol. 28 (1976): 671.
- [20] ดุสิต เครื่องงาม, และคณะ, เซลล์แสงอาทิตย์ชนิดอะมอร์ฟิซิลิคอน. รายงานการวิจัยพัฒนา และวิศวกรรมฉบับสมบูรณ์. ศูนย์เทคโนโลยีอิเล็กทรอนิกส์และคอมพิวเตอร์แห่งชาติ. (2535): 63.



สถาบันวิทยบริการ
จุฬาลงกรณ์มหาวิทยาลัย

LIST OF PUBLICATIONS

1. D. Kruangam, F. Wongwan, T. Chutarasok, K. Chirakawikul, S. Panyakeow, “Amorphous photocoupler consisting of a-SiC:H thin film light emitting diode and a-SiGe:H thin film photodiode”, Journal of Non-Cryst. Solids 226-269(2000) 1241-1246.
2. Fontip Wongwan, Tula Chutarosaka, Kriangkrai Chirakawikul, Dusit Kruangam and Somsak Panyakeow, “Fabrication of Amorphous Silicon Germanium Thin Film Photodiode for Infrared Light”, Proceedings of the 22th conference on electrical engineering, Kasetsart University (2-3 December 1999).
3. Tula Chutarosaka, Fontip Wongwan, Kriangkrai Chirakawikul, Dusit Kruangam and Somsak Panyakeow, “A Study of Basic Properties of Hydrogenated Amorphous Silicon Germanium Thin Films”, Proceedings of the 22th conference on electrical engineering, Kasetsart University (2-3 December 1999).



สถาบันวิทยบริการ
จุฬาลงกรณ์มหาวิทยาลัย

APPENDIX



สถาบันวิทยบริการ
จุฬาลงกรณ์มหาวิทยาลัย

Amorphous Silicon Germanium Solar Cell

1 Introduction

In chapters 2-6, a series of study on the preparation of a-SiGe:H and applications of a-SiGe:H as the active layer in an amorphous thin film photodiode as well as in an amorphous thin film photocoupler have been described. However, it is interesting to check the possibility of the application of a-SiGe:H as the active layer in an amorphous silicon based solar cells. In this chapter, the result of a preliminary experiment on the application of a-SiGe:H in a solar cell is presented.

Hydrogenated amorphous silicon (a-Si:H) solar cells have been firstly developed by Wronski and Carlson in 1976 [19]. In Thailand the first a-Si:H solar cell was fabricated at the Semiconductor Device Research Laboratory in 1989 and the conversion efficiency was about 7% [20]. Since a-Si:H has the optical energy gap around 1.7 – 1.8 eV, the a-Si:H solar cells have the maximum collection efficiency at the wavelength around 550 – 600 nm. The longest wavelength that a-Si:H solar cells respond to the solar light is about 800 nm. One method to improve the conversion efficiency of amorphous silicon based solar cells is to design solar cells that can absorb the infrared light having the wavelength longer than 800 nm and stacked the visible light solar cells and the infrared light solar cells as a tandem structure (vertical multi-layers).

As described in chapters 2-6, hydrogenated amorphous silicon germanium (a-SiGe:H) is one of the amorphous silicon alloys that has small optical energy gap and has reasonable photo-conductivity. Therefore, it is interesting to study the fabrication technology of a-SiGe:H based solar cells. In this chapter, the fabrication of amorphous solar cells having a-SiGe:H as an active layer will be described.

2 Structure and Fabrication of a-SiGe:H Solar Cells

The structure of a-SiGe:H solar cell fabricated in the work is shown in Figure 1. The p-a-SiC:H ($E_{opt} = 2.0$ eV) was used as the front wide window layer. The n-microcrystalline Si:H ($E_{opt} = 1.9$ eV) was used as the back n-layer. Glass/ITO/SnO₂ was used as the substrate. Aluminum was deposited to the top as the back contact electrode. The thickness of each layer is mentioned in the Figure. Some preparation conditions by the glow discharge plasma CVD method is shown in Table 1. Figure 2 shows an example of the fabricated a-SiGe:H solar cells. Figure 3 shows the configuration of the measurement system of the conversion efficiency of solar cells using a computer and solar simulator.

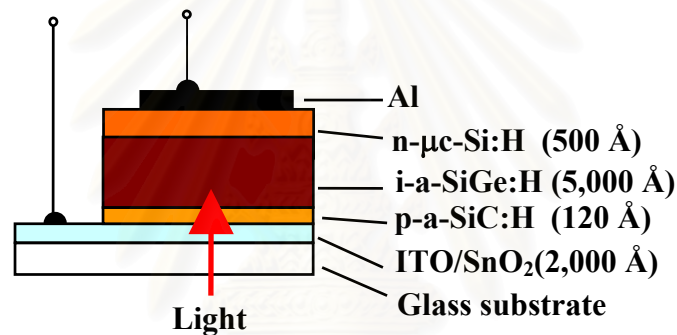


Figure 1 Structure of a-SiGe:H thin film solar cell.

Table 1 Preparation conditions of a-SiGe:H thin film solar cells by the glow discharge plasma CVD.

| Layers | Thickness (Å) | Substrate temperature (°C) | Gases |
|------------|---------------|----------------------------|---|
| p-a-SiC:H | 200 | 190 | SiH ₄ +B ₂ H ₆ +H ₂ |
| i-a-SiGe:H | 5,000 | 250 | SiH ₄ +GeH ₄ +H ₂ |
| n-μc-Si:H | 500 | 190 | SiH ₄ +PH ₃ +H ₂ |

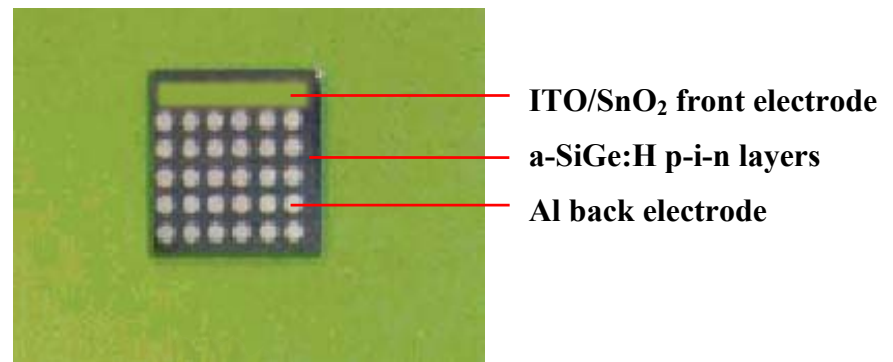


Figure 2 Photograph of the example of a-SiGe:H thin film solar cells.

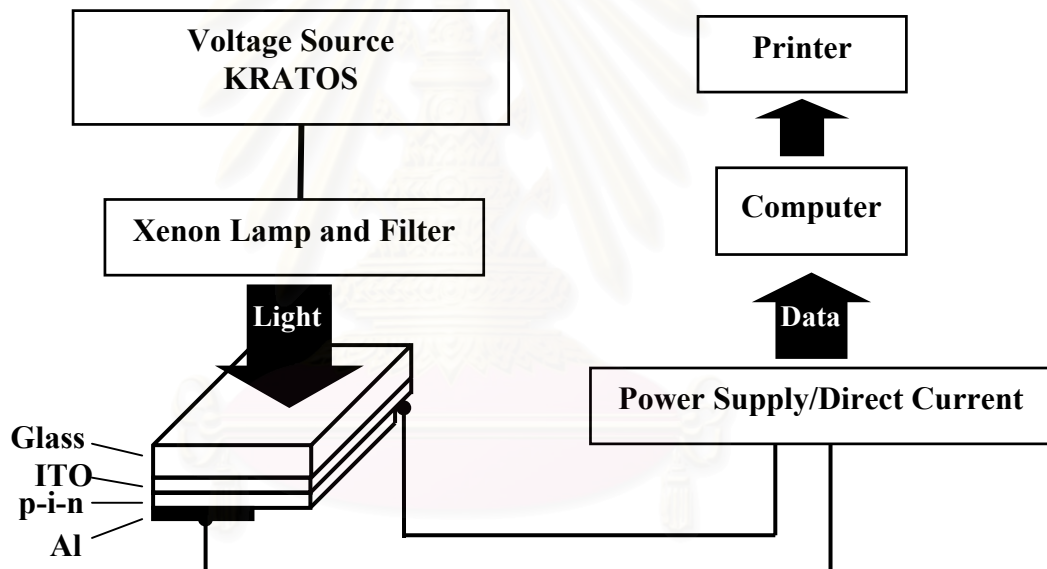


Figure 3 Configuration of the measurement system of the conversion efficiency of solar cells using a computer and a solar simulator.

3 Results

The output characteristics of the a-SiGe:H solar cell are as follows:

| | |
|--------------------------------|---------------------------|
| Conversion Efficiency | = 0.25 % |
| Fill factor | = 22.05 % |
| Short circuit current J_{sc} | = 2.25 mA/cm ² |
| Open circuit volatge V_{oc} | = 0.51 V. |

The very low output characteristics of the a-SiGe:H solar cell are due to the low photo-conductivity of the a-SiGe:H. However, it is expected that at the technology level, if the thickness of the i-a-SiGe:H layer is optimized, the conversion efficiency of the a-SiGe:H solar cell will be improved.

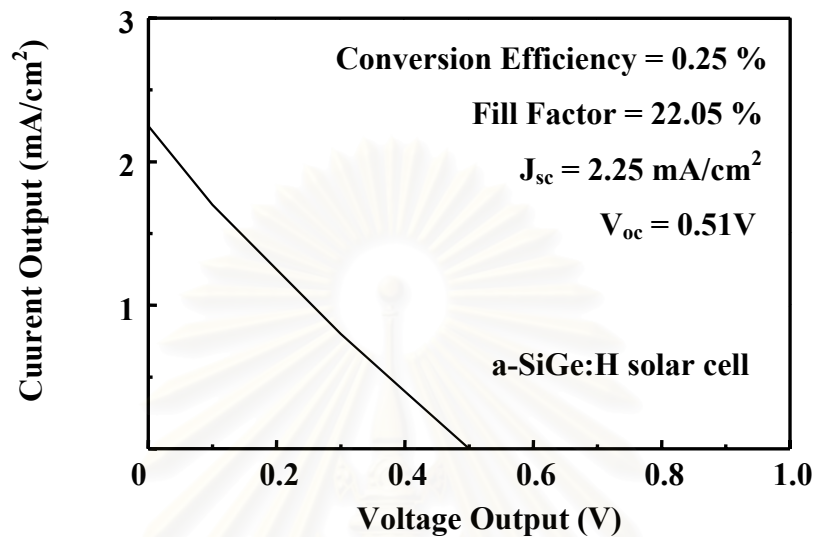


Figure 4 Relationship between $J(\text{mA}/\text{cm}^2)$ and Voltage of solar cell which i-layer was a-SiGe:H of the condition $\text{SiH}_4:\text{GeH}_4 = 50:5$.

Summary

- 1) An a-SiGe:H solar cell was fabricated by the glow discharge plasma CVD method.
- 2) The output characteristics of the preliminary experiment are as follows: conversion efficiency = 0.25%, fill factor = 22.05 %, $J_{sc} = 2.25 \text{ mA}/\text{cm}^2$ and $V_{oc} = 0.51 \text{ V}$.
- 3) The poor properties of the a-SiGe:H thin film solar cell were due to the high density of dangling bonds in the i-a-SiGe:H and the interface states between the p-a-SiC:H and i -a-SiGe:H layer.
- 4) The conversion efficiency is expected to be improved through the optimization of the thickness of the a-SiGe:H layer. (There are also some other technologies).

APPENDIX



สถาบันวิทยบริการ
จุฬาลงกรณ์มหาวิทยาลัย

Amorphous Silicon Germanium Solar Cell

1 Introduction

In chapters 2-6, a series of study on the preparation of a-SiGe:H and applications of a-SiGe:H as the active layer in an amorphous thin film photodiode as well as in an amorphous thin film photocoupler have been described. However, it is interesting to check the possibility of the application of a-SiGe:H as the active layer in an amorphous silicon based solar cells. In this chapter, the result of a preliminary experiment on the application of a-SiGe:H in a solar cell is presented.

Hydrogenated amorphous silicon (a-Si:H) solar cells have been firstly developed by Wronski and Carlson in 1976 [19]. In Thailand the first a-Si:H solar cell was fabricated at the Semiconductor Device Research Laboratory in 1989 and the conversion efficiency was about 7% [20]. Since a-Si:H has the optical energy gap around 1.7 – 1.8 eV, the a-Si:H solar cells have the maximum collection efficiency at the wavelength around 550 – 600 nm. The longest wavelength that a-Si:H solar cells respond to the solar light is about 800 nm. One method to improve the conversion efficiency of amorphous silicon based solar cells is to design solar cells that can absorb the infrared light having the wavelength longer than 800 nm and stacked the visible light solar cells and the infrared light solar cells as a tandem structure (vertical multi-layers).

As described in chapters 2-6, hydrogenated amorphous silicon germanium (a-SiGe:H) is one of the amorphous silicon alloys that has small optical energy gap and has reasonable photo-conductivity. Therefore, it is interesting to study the fabrication technology of a-SiGe:H based solar cells. In this chapter, the fabrication of amorphous solar cells having a-SiGe:H as an active layer will be described.

2 Structure and Fabrication of a-SiGe:H Solar Cells

The structure of a-SiGe:H solar cell fabricated in the work is shown in Figure 1. The p-a-SiC:H ($E_{opt} = 2.0$ eV) was used as the front wide window layer. The n-microcrystalline Si:H ($E_{opt} = 1.9$ eV) was used as the back n-layer. Glass/ITO/SnO₂ was used as the substrate. Aluminum was deposited to the top as the back contact electrode. The thickness of each layer is mentioned in the Figure. Some preparation conditions by the glow discharge plasma CVD method is shown in Table 1. Figure 2 shows an example of the fabricated a-SiGe:H solar cells. Figure 3 shows the configuration of the measurement system of the conversion efficiency of solar cells using a computer and solar simulator.

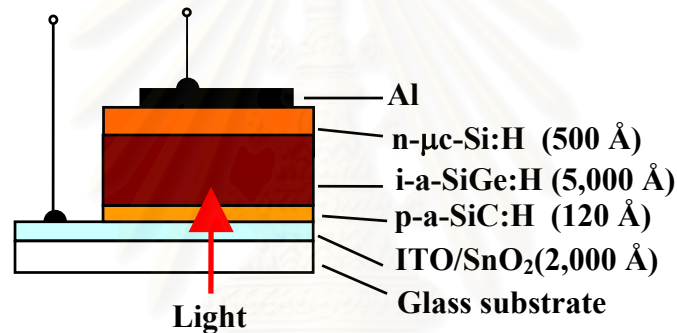


Figure 1 Structure of a-SiGe:H thin film solar cell.

Table 1 Preparation conditions of a-SiGe:H thin film solar cells by the glow discharge plasma CVD.

| Layers | Thickness (Å) | Substrate temperature (°C) | Gases |
|------------|---------------|----------------------------|---|
| p-a-SiC:H | 200 | 190 | SiH ₄ +B ₂ H ₆ +H ₂ |
| i-a-SiGe:H | 5,000 | 250 | SiH ₄ +GeH ₄ +H ₂ |
| n-μc-Si:H | 500 | 190 | SiH ₄ +PH ₃ +H ₂ |

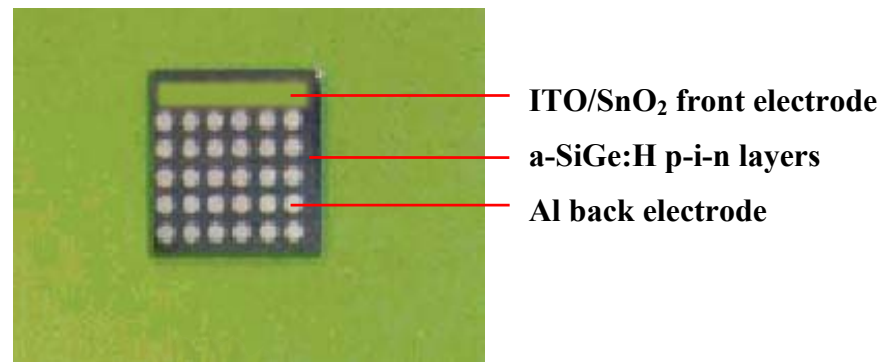


Figure 2 Photograph of the example of a-SiGe:H thin film solar cells.

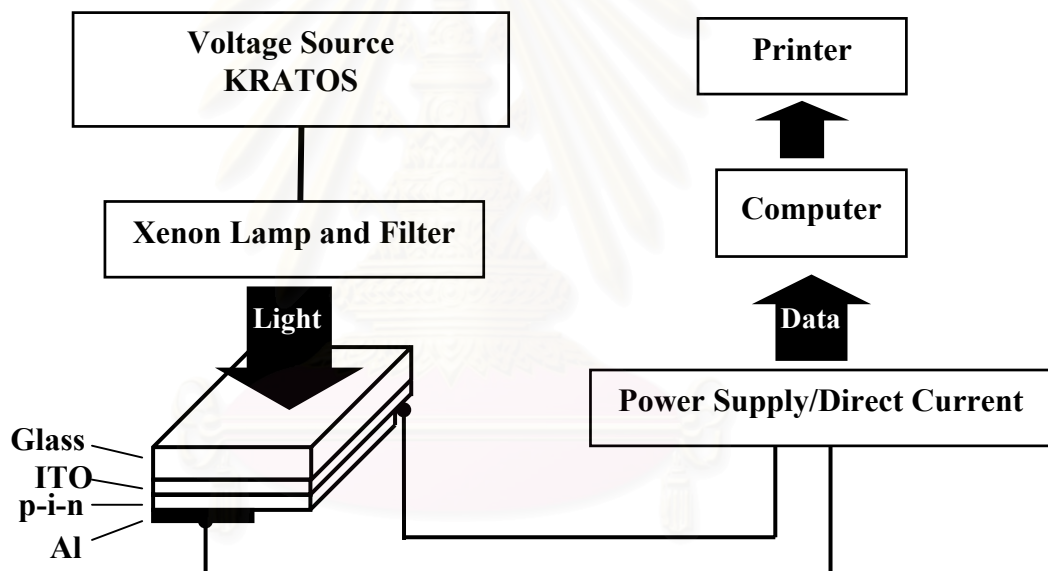


Figure 3 Configuration of the measurement system of the conversion efficiency of solar cells using a computer and a solar simulator.

3 Results

The output characteristics of the a-SiGe:H solar cell are as follows:

| | |
|--------------------------------|---------------------------|
| Conversion Efficiency | = 0.25 % |
| Fill factor | = 22.05 % |
| Short circuit current J_{sc} | = 2.25 mA/cm ² |
| Open circuit volatge V_{oc} | = 0.51 V. |

The very low output characteristics of the a-SiGe:H solar cell are due to the low photo-conductivity of the a-SiGe:H. However, it is expected that at the technology level, if the thickness of the i-a-SiGe:H layer is optimized, the conversion efficiency of the a-SiGe:H solar cell will be improved.

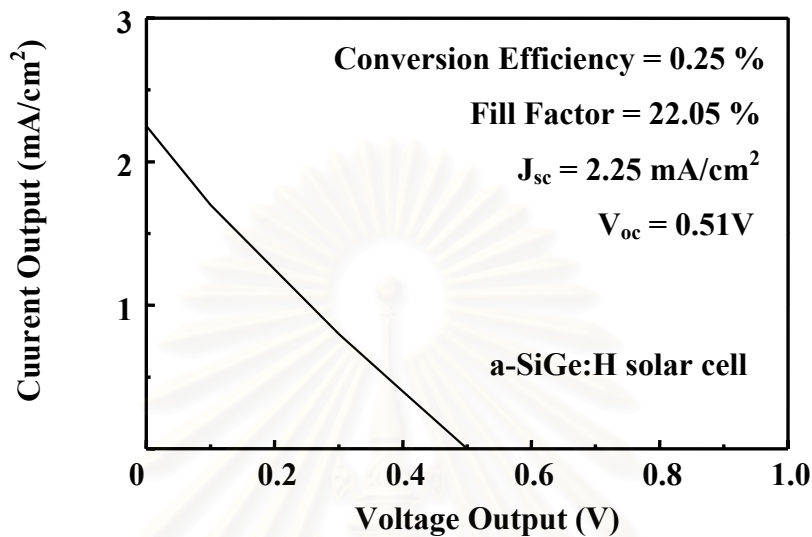


Figure 4 Relationship between $J(\text{mA}/\text{cm}^2)$ and Voltage of solar cell which i-layer was a-SiGe:H of the condition $\text{SiH}_4:\text{GeH}_4 = 50:5$.

Summary

- 1) An a-SiGe:H solar cell was fabricated by the glow discharge plasma CVD method.
- 2) The output characteristics of the preliminary experiment are as follows: conversion efficiency = 0.25%, fill factor = 22.05 %, $J_{sc} = 2.25 \text{ mA}/\text{cm}^2$ and $V_{oc} = 0.51 \text{ V}$.
- 3) The poor properties of the a-SiGe:H thin film solar cell were due to the high density of dangling bonds in the i-a-SiGe:H and the interface states between the p-a-SiC:H and i -a-SiGe:H layer.
- 4) The conversion efficiency is expected to be improved through the optimization of the thickness of the a-SiGe:H layer. (There are also some other technologies).

BIOGRAPHY

Miss Fontip Wongwan was born in Petchaboon Province, Thailand on March 14, 1977. She received the Bachelor Degree of Engineering in Electronics Engineering from King Mongkut Institute of Technology Ladkrabang (KMITL) in March 1997. She entered the Graduate School of Chulalongkorn University in June 1997 as a student of the Semiconductor Device Research Laboratory. Her current interests are in the field of amorphous semiconductors, solar cell technology and energy conservation.



สถาบันวิทยบริการ
จุฬาลงกรณ์มหาวิทยาลัย